1-29-2018 2:30 PM

A High Gain DC-DC Full-Bridge Converter

Prashanth Prabhu, *The University of Western Ontario*

Supervisor: Moschopoulos, Gerry, *The University of Western Ontario*

A thesis submitted in partial fulfillment of the requirements for the Master of Engineering Science degree in Electrical and Computer Engineering

Abstract

High gain DC-DC converters have become increasingly popular in recent years as there is greater need to interface low voltage DC sources such as solar cells and batteries with much higher voltage DC buses. A new high gain DC-DC converter with high gain, galvanic isolation and an integrated passive snubber network is proposed in the thesis. In the thesis, the general operation of the converter is discussed, its modes of operation are explained and its features are reviewed. The design of the converter is then discussed and a set of general guidelines that can be used in the design are presented. The feasibility of the converter is confirmed with experimental results obtained from a prototype converter.

Keywords

power converter, DC-DC converter, high gain converter, switch-mode power converter, switch-mode power supply, boost converter.

Acknowledgments

First and foremost, I would like to express my sincere gratitude to my advisor, Dr. Gerry Moschopoulos whose has supported me throughout my research with his everlasting patience and knowledge. I attribute the level of my Master's degree to his encouragement and effort and without him this thesis would not have been completed or written. One simply could not wish for a better or friendlier supervisor.

Furthermore, I would also like to express special thanks to Ms. Michelle Wagler, the Administrative Officer and Ms. Stephanie Tigert, the Graduate Coordinator at the Department of Electrical and Computer Engineering at University of Western Ontario for their great help with all the administrative work throughout my time in the M.E.Sc. program.

Also, I would like to recognize the guidance and support provided by fellow researchers and students at the Power Engineering lab, Dr. Mona El Dahb, Adel Abosnina, Javad Khodabakhsh, Ramtin Rasoulinezhad, and Adel Alganidi. Their insights and expertise in power electronics helped me immensely in my graduate studies and I was blessed to work with such a friendly and cheerful group of fellow students.

Finally, I would like to thank my parents for allowing me to realize my own potential. All the support they have provided me over the years was the greatest gift anyone has ever given me.

Table of Contents

List of Tables

List of Figures

List of Appendices

Chapter 1

1 Introduction

1.1 Introduction to Power Electronics

Power electronics is the field of electrical engineering that focuses on the use of solid state electronics to convert power from one form to another. The objective of a power electronic converter circuit is typically to match the voltage level of the load with an available source that is different in form and/or amplitude. Power electronic converters thus serve as the interface between various power sources and loads and are a vital part of modern electronics.

As an integral part of today's energy systems involving renewable resources, applications of power electronics are expanding exponentially. It would not be possible to build modern computers, phones, hybrid vehicles, solar panels, wind turbines, LED lighting and many similar devices without power electronic technologies. Key aspects of power electronics include the use of high power semiconductor devices, the application of magnetic devices for energy storage, and the implementation special control methods for complex non-linear systems. A block diagram of a typical power electronic system is shown in Figure 1.1.

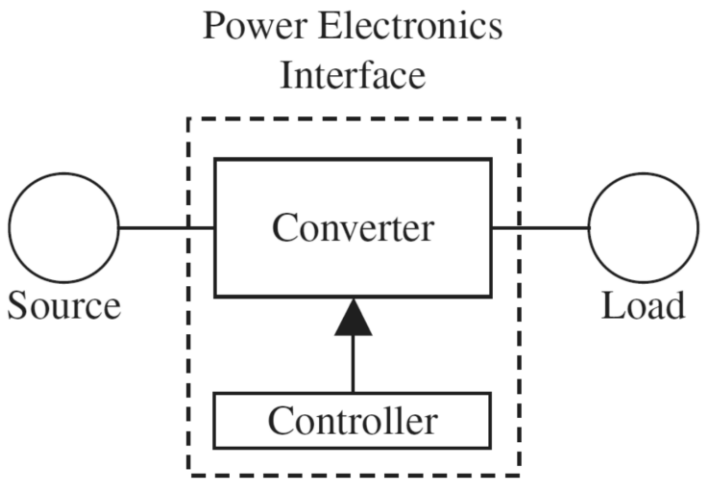

Figure 1.1: Power electronics interface [1]

Power electronic circuits can be broadly classified based on the type of voltage they convert as follows:

- ***AC/DC power converters***, commonly referred to as rectifiers, aim to convert an alternating current (AC) voltage input to an appropriate direct current (DC) voltage output based on the load. Example of this type of converter would be a laptop charger.

- ***DC/AC converters***, which are also called inverters, convert a DC input to an equivalent AC signal as required by the load. These converters are commonly found in a household uninterruptible power supply (UPS).

- ***DC/DC converters***, which are used when the load required a regulated DC voltage or current but the source is at a different or unregulated value. An example of this converter is the buck converter powering a USB port.

- ***AC/AC converters***, which are used to transform a AC signal to another AC signal with a different magnitude or frequency depending on the requirement of the load being driven by the converter. Cyclo-converters used in cement kilns are an example of AC/AC power converters.

Another classification of power converters is based on whether the converter is interfaced with a voltage or current source. Power converters can therefore be considered to be voltage source or current source converters. Both types are described in further detail below,

A voltage source converter is fed from a DC voltage source, usually filtered by a relatively large capacitor connected in parallel. In the example shown in Figure 1.2, a DC voltage source feeds the main converter circuit, which can be a generic topology that converts the power from one form to another as required. The DC voltage source is usually a DC capacitor fed by a battery, fuel cell stack, or diode rectifier.

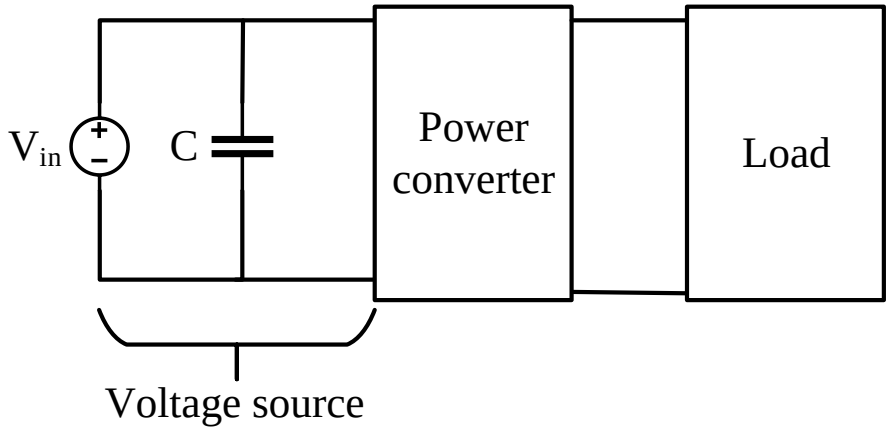

Figure 1.2: Voltage sourced converter [2]

In contrast, a current source converter is fed from a DC current source, which in most cases is implemented by connecting a DC voltage source in series with a rather large inductor, as shown in Figure 1.3. Along with the inductor, the DC voltage source forms a current source that provides a stiff current for the power converter

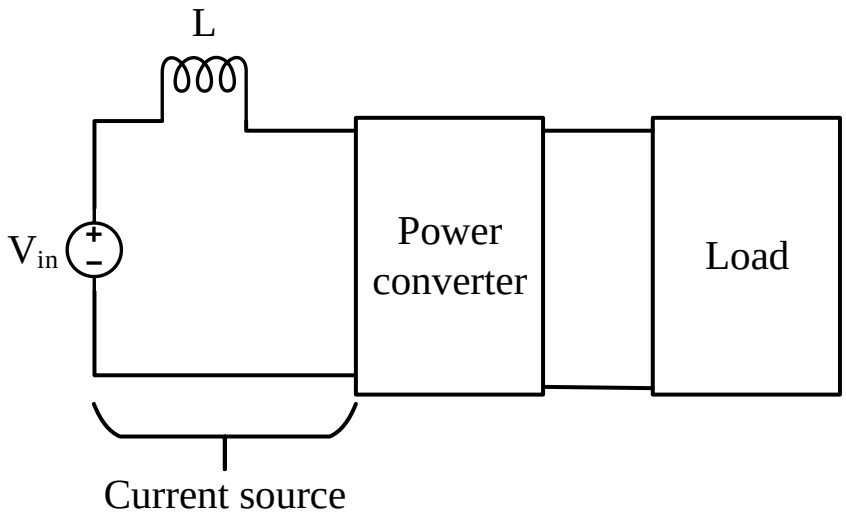

Figure 1.3: Current sourced converter

In general, voltage source converters usually step-down voltage and current source converters boost voltage; thus, voltage source and current source converters are capable of performing different power conversions as they have their own advantages and disadvantages.

1.2 Power electronic devices

The semiconductor devices that are typically used in power converter topologies are diodes and transistors. In high frequency power converters, devices that are used typically used include fast recovery diodes, Schottky diodes, metal–oxide–semiconductor field-effect transistors (MOSFETs), and insulated-gate bipolar transistors (IGBTs). These devices can be considered to be electronic switches and are characterized by their ability to have two states, on and off, ideally either a short circuit or an open circuit.

Diodes are uncontrollable switches as they are on when forward-biased and off when they are reverse-biased; this characteristic cannot be controlled by an external input. Also, current cannot be interrupted in a diode and some action external to the diode must be taken to divert current away from it and make it reverse-biased. On the other hand, MOSFETs and IGBTs are controllable switches and can be tuned on or off based on the signal fed to the device.

In this thesis, the main power semiconductor devices that will be considered are fact-recovery diodes and MOSFETs. The basic characteristic of each device is discussed below.

1.2.1 Diodes

Power diodes are the simplest electronic switches used in switched mode power supplies, they turn on and off based on the voltage applied across their anode-cathode terminals. A diode is turned on when its anode-cathode voltage exceeds its forward voltage drop and it is turned off when this voltage is lower than the forward voltage drop (i.e. when the anode-cathode voltage is negative); current flows from anode to cathode. A key difference among various types of diodes arises from their reverse-recovery characteristics, which is related to the amount of time needed for a diode to stop conducting current once the polarity of the anode-cathode voltage is reversed. Due to its construction, a typical diode cannot turn off instantaneously but also allows current to flow in the negative direction (cathode to anode) for some time before it finally turs off. Examples of diodes with reverse-recovery characteristics are shown in Figure 1.4, with Figure 1.4(a) showing the characteristic of a slow- recovery diode and Figure 1.4(b) showing that of a fast-recovery diode. Fast-

recovery diodes are preferred over slow-recovery diodes in power converters operating with high switching frequencies.

The main issues with reverse-recovery current are: (a) losses due to voltage and current overlap; (b) the generation of noise if the characteristic is sharp; (c) current stresses on other components if the reverse-recovery current is high. Reverse-recovery current can be reduced if current is gradually transferred away from a diode as it allows time for the diode to turn off.

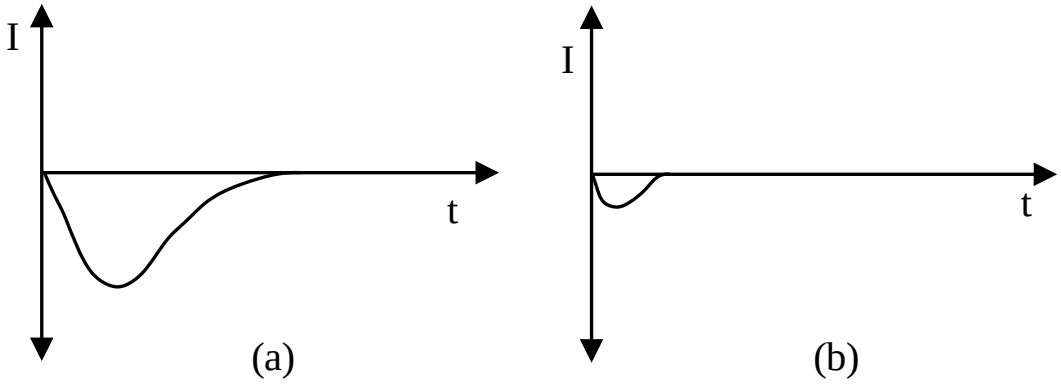

Figure 1.4: Comparison of diode recovery characteristics [3]

1.2.2 MOSFET

The metal–oxide–semiconductor field-effect transistor is the most common electronic switch used for higher switching frequency based switched mode power supplies. It has three terminals - gate, drain and source - as shown in Figure 1.5.

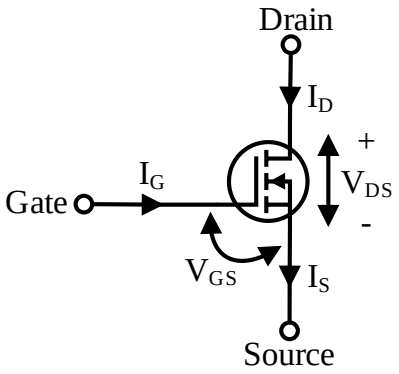

Figure 1.5: MOSFET symbol

The switch is on when current is fed to the gate and its gate source capacitance is charged to a threshold voltage, V_{th}, which creates a field that opens the drain source channel and allows current to flow from drain to source. Current, however, does not have to be continuously fed to the gate to keep the device on; the device is on as long as the voltage across the gate-source capacitance V_{gs} is greater than V_{th} so that the electrical field required to keep the channel open is maintained. This allows the MOSFET to have a fast switching speed as the field can be generated or removed very quickly, thus making the MOSFET the device of choice for applications where high frequency switching is required.

With the need for modern power converters to be smaller in size, there has been a push to increase the frequency at which they operate as this this would shrink the passive magnetic elements like inductors and transformers.

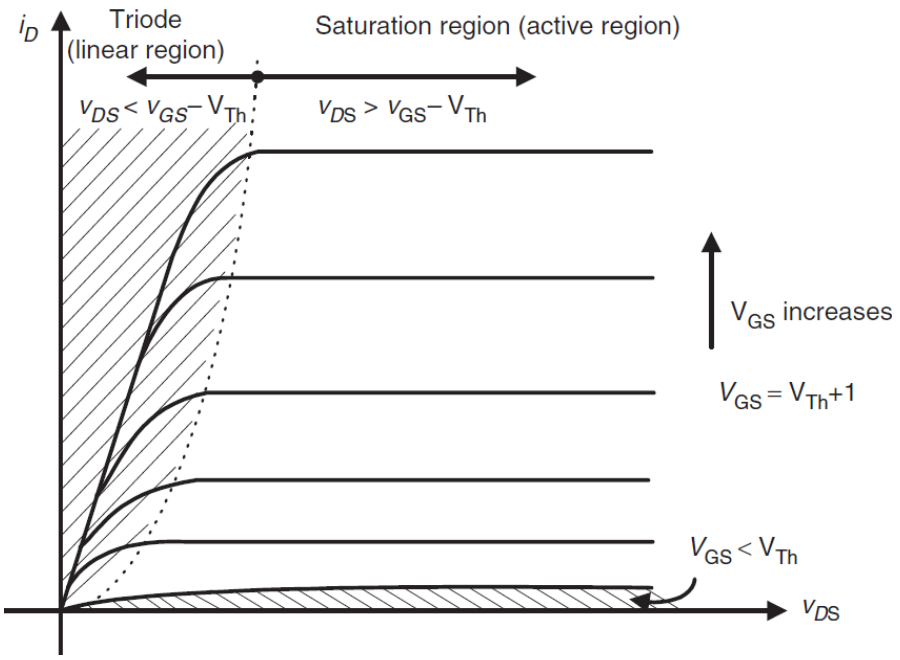

Figure 1.6: MOSFET IV characteristics [1]

The MOSFET has three main regions of operation: triode, saturated, and cut-off. These regions are shown in the drain current / drain-source voltage (I-V) characteristics of a MOSFET shown in Figure 1.6. Since controllable semiconductor devices in almost all

power electronics applications function as switches that either completely on or off, a MOSFET in a power converter operates in the triode region or in the cut-off region.

When a MOSFET is on, however, it is not an ideal switch as it has some resistance $R_{ds,\ on}$ between the drain and source that contributes to energy loss when current flows through the device. In power applications with high switching frequencies, MOSFET's are the device of choice because of their fast switching speed and high impedance gate, which requires the application or removal of a small voltage and charge to facilitate a switching action.

1.3 Literature review

The main focus of this thesis will be on DC/DC converters with high voltage gains. DC-DC power converters with high voltage gains [4]–[8] have become more widely used in recent years due to the increase in applications where such gains are required. Applications that drive this technology include renewable energy systems fed by photovoltaic (PV) solar cells and fuel cells that produce low input voltages, and power architectures where batteries are used. In such applications, these low DC voltages need to be converted to much higher DC voltages to supply downstream converters such as point-of-use power supplies and inverters.

An example of an renewable energy system is shown in Figure 1.7. In this system, the low input DC source, whether it consists of photovoltaic (PV) solar cells or a fuel cell stack it is stepped up to a much higher DC level that is subsequently converted to a three-phase AC voltage that can be fed to the utility grid. This thesis will propose a new high DC/DC converter that makes use of the following concepts:

- Boost (step-up) converters
- Snubbers
- Z-source converters

This section serves as a literature review of these key concepts in preparation for the new high-gain DC-DC converter that will be proposed in this thesis.

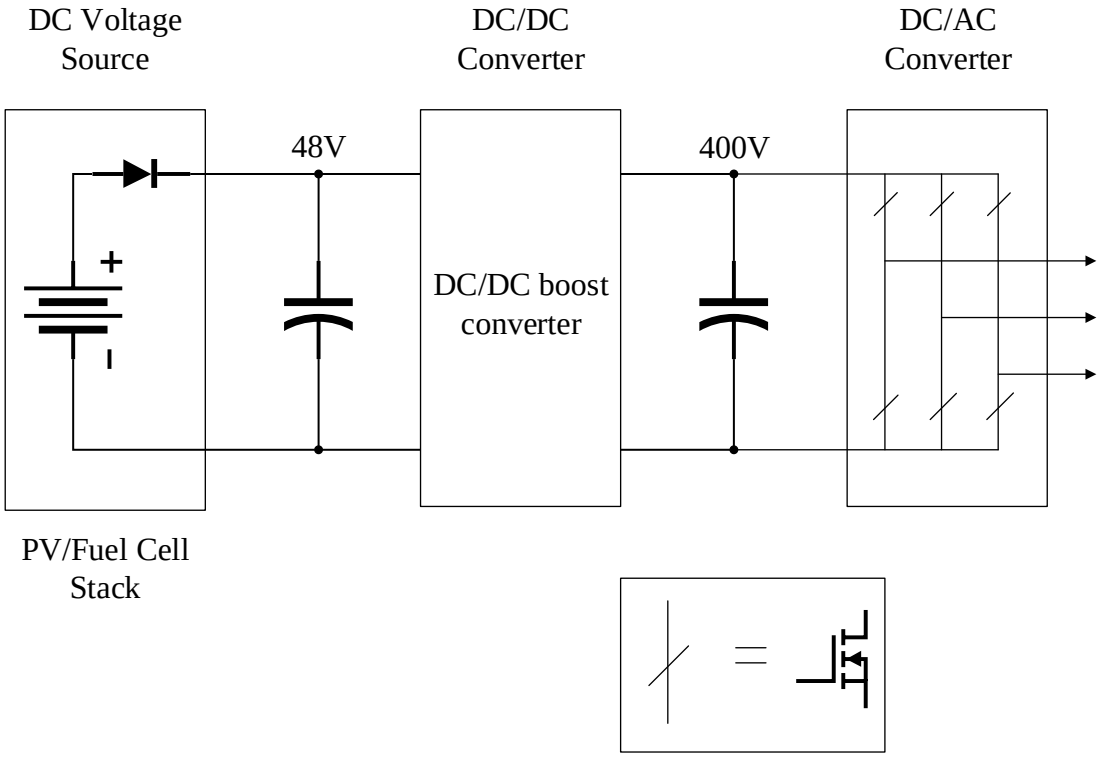

Figure 1.7: Two stage power conversion system for PV and fuel cell applications

1.3.1 Boost converters

The proposed converter is a boost-type converter; therefore, boost converters are reviewed in this section. A boost converter is a converter that has output voltage that is higher than its input voltage.

1.3.1.1 Conventional boost converter

The conventional boost converter is the simplest power converter that can be used to increase DC voltage; a diagram of this circuit is shown in Figure 1.8. It is a simple topology with one semiconductor switch, usually a MOSFET as described above, a diode, typically a fast-recovery diode, an input inductor and an output filter capacitor to smooth the output voltage so that it approximates an ideal DC voltage waveform.

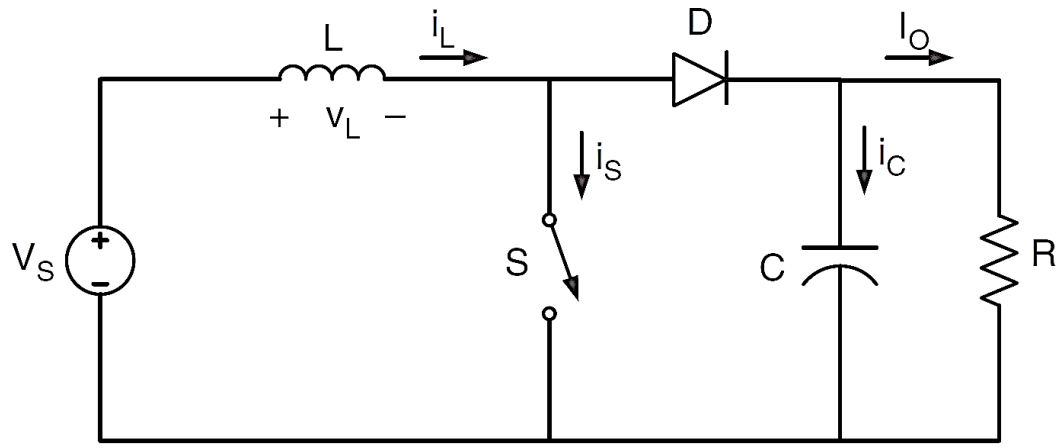

Figure 1.8: Boost converter schematic [9]

When the switch is turned on, the diode does not conduct and the inductor is energized as the full input voltage is placed across it. When the switch is turned off, the diode conducts and the energy that was stored in the inductor is transferred to the output. The key modes of operation of this converter are shown in Figures 1.9 and 1.10.

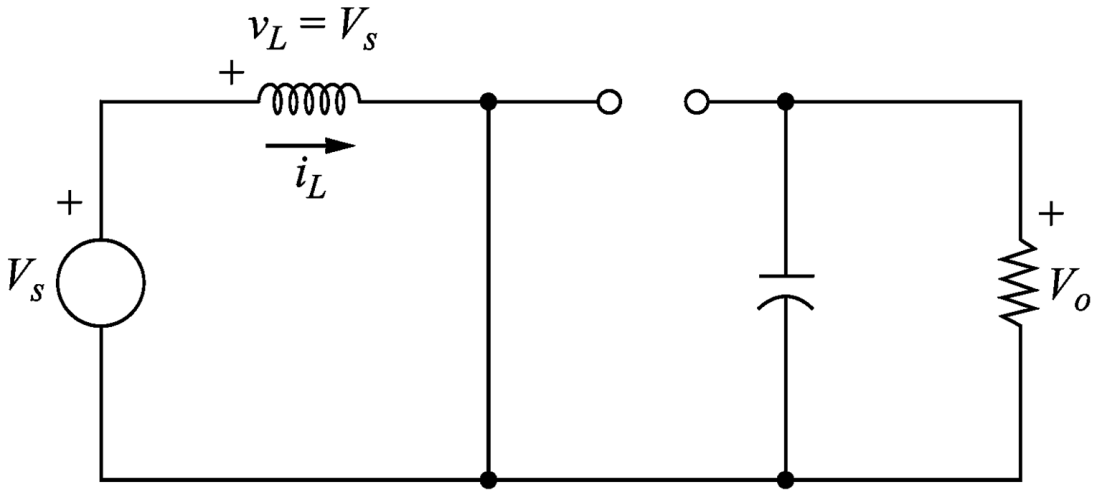

Figure 1.9: Equivalent circuit during shoot through mode [10]

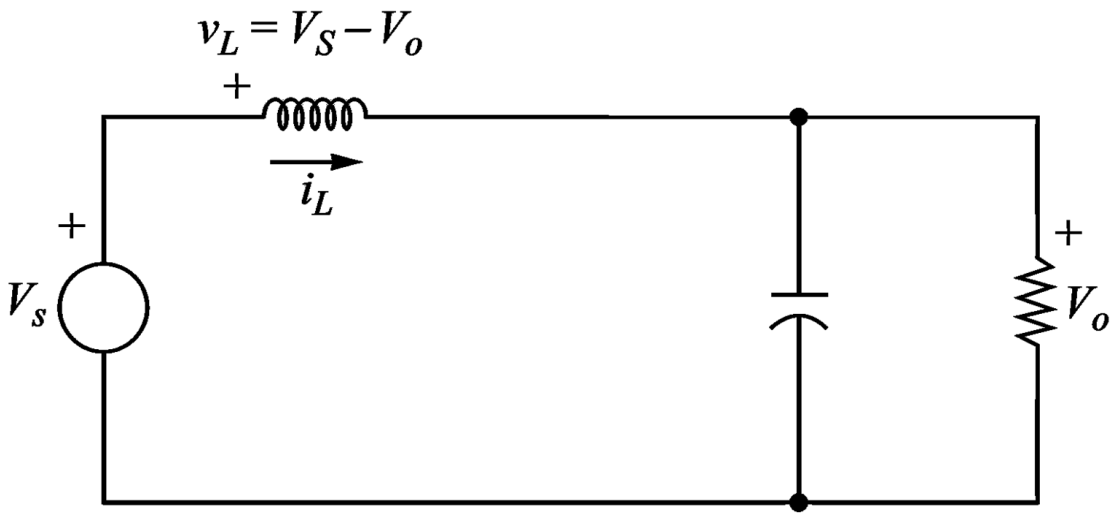

Figure 1.10: Equivalent circuit during energy transfer mode [10]

Key converter waveforms are shown in Figures 1.11 and 1.12 [10]. Figure 1.11(a) shows the voltage across the input inductor. It can be seen that this voltage is positive when the switch is on and negative when the switch is off as the voltage across the inductor is the difference between the output voltage and the input voltage. Figure 1.11(b) is the input inductor current; which rises when the switch is on and positive voltage is applied across the inductor and falls when the switch is off and negative voltage is applied across the inductor.

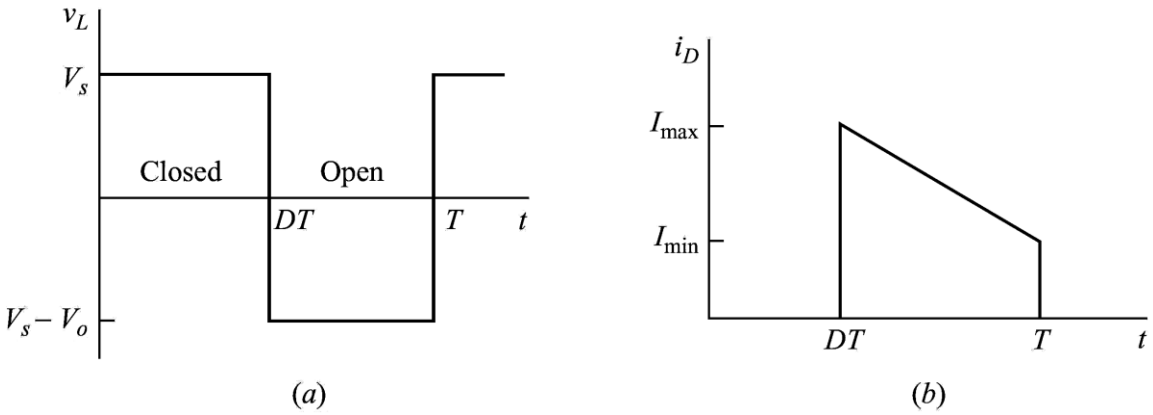

Figure 1.11: Boost converter waveforms (a) Inductor voltage; (b) Inductor current

Figure 1.12(a) is the current flowing through the diode, which is the falling portion of the input inductor current waveform. Figure 1.12(b) is the current through the output capacitor, which is the diode current minus the DC current fed to the output load.

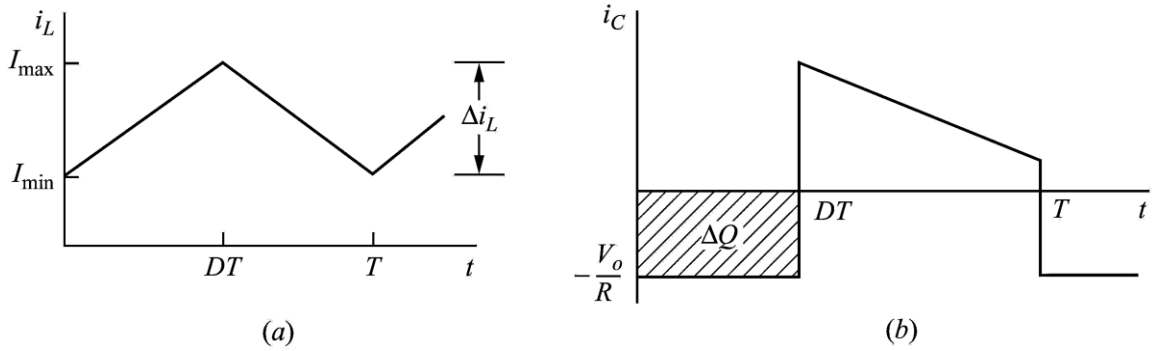

Figure 1.12: Boost converter waveforms (a) Diode current; (b) Capacitor current

The gain of the converter, its output voltage to input voltage ratio is dependent on its duty cycle D, which is the ratio of switch on-time to the length of the switching cycle (or period). It can be expressed as follows:

$$V_o = \frac{V_s}{(1-D)} \tag{1.1}$$

As the duty cycle ratio is increased, the denominator of equation 1.1 becomes smaller, resulting in a larger output voltage. The conventional pulse-with modulated (PWM) boost converter, however, [11]–[14] is not suitable for high-gain applications and it can only achieve very high gains if its duty ratio is almost one, which is impractical.

1.3.1.2 Current-fed full bridge boost converter

Isolated power converters with a transformer in their topologies have a number of advantages over non-isolated topologies such as the conventional boost converter, including [1]:

- The avoidance of extreme duty-cycles: If the DC/DC voltage conversion gain is large, then a transformer can be used to help step up voltage instead of relying on extreme values of duty cycle, which are impractical.

- Safety: To avoid shock hazards, it is common practice to try to keep high voltages and low voltages isolated from each other. In a high-gain converter, this means isolating the high output voltage from the low source voltage.

An example of an isolated converter is the current-fed full-bridge converter shown in Figure 1.13. This converter is usually used at higher power applications in the range of 500W and above. It consists of four switches, a transformer with a center-tapped secondary winding, two output diodes, an output filter capacitor, and an input inductor that is sufficiently large to form a current source with the input source voltage.

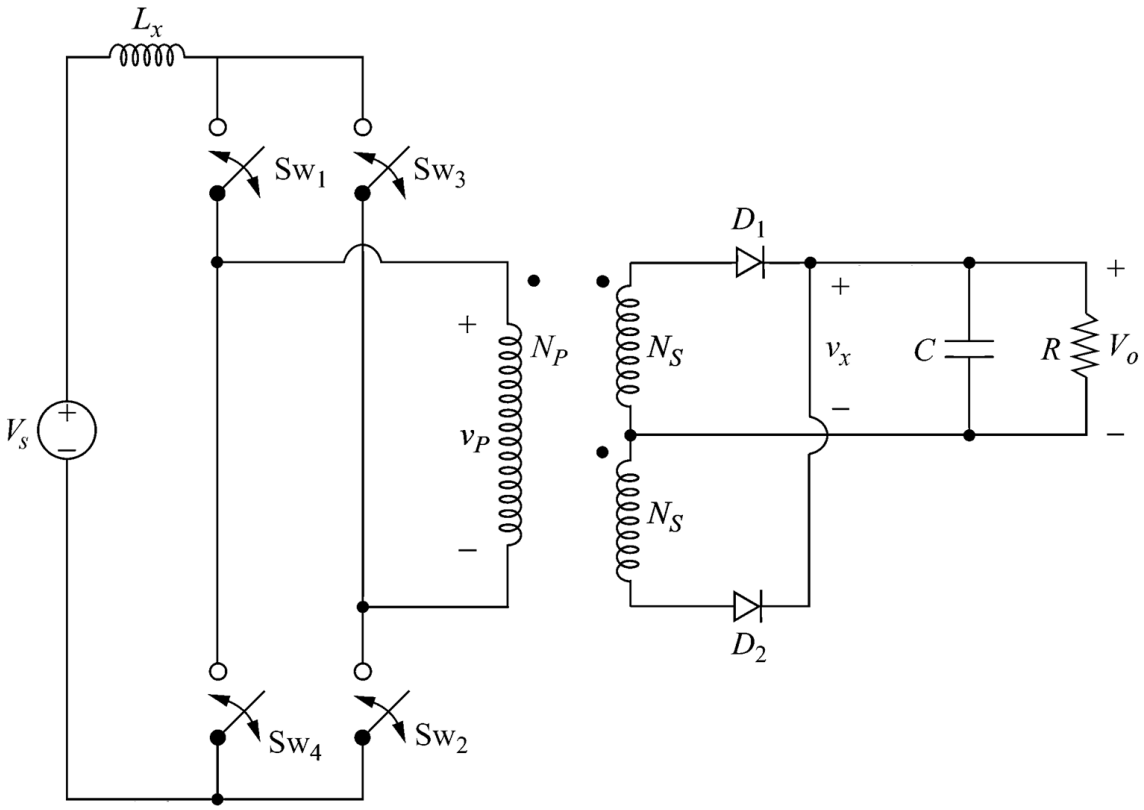

Figure 1.13: Schematic of current fed full bridge boost converter

This converter uses pulse-width modulation (PWM) to vary the duty cycle so that the required voltage gain is obtained. The on/off gate pulses of four switches are shown in Figure 1.14.

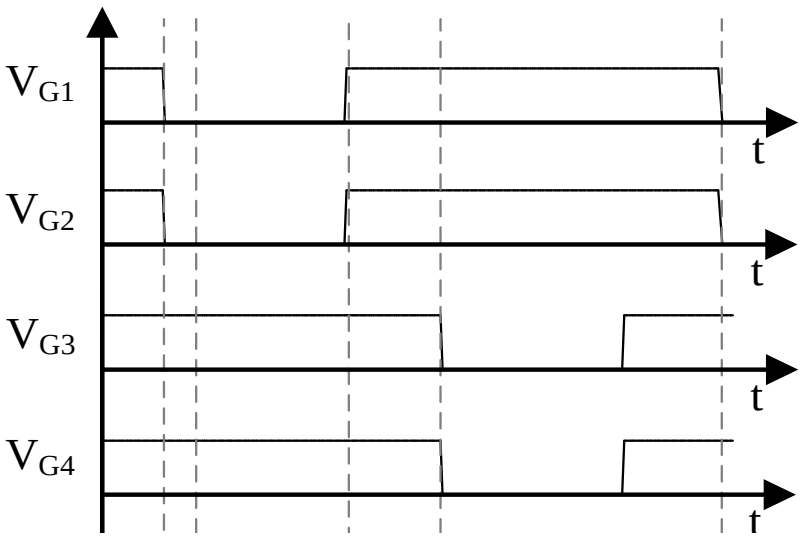

Figure 1.14: Typical gate signal waveforms

The converter's voltage gain is similar to that of the boost converter and can be expressed as

$$V_o = \frac{nV_s}{(1-D)} \tag{1.2}$$

where n is the turns ratio.

There are two principal modes of operation in this converter for each half cycle:

Mode 1 (0 ≤ t < DT): This operation mode is started when all the switches are turned on. The energy is stored in inductor L and because it's voltage is constant (inductor L voltage is equal to V_s), it's current increases linearly. In this mode of operation, output capacitor (C) is being discharged as it supplies current to the load. This mode is a typical shoot-through mode.

Mode 2 (DT ≤ t ≤ T): This operation mode is started when switches S_1 and S_2 are turned on and switches S_3 and S_4 are turned off. When this happens, the inductor voltage becomes equal to $V_s - V_o / n$ and because this is a constant negative voltage, inductor current decreases linearly in this operation mode. Energy is transferred to the output and the

capacitor is charged because the diode current supplies the capacitor and the load; this is an energy transfer mode.

1.3.1.3 High step-up converter with coupled inductor

Coupled inductors can be considered to be transformers, as they can be implemented with two or more windings wrapped on a common magnetic core but their primary and secondary windings are not isolated.

The main advantage of using coupled inductors in high-gain DC/DC converters is that even greater gains can be achieved than with transformers as primary voltage can be added to secondary voltage; the main disadvantage is that high and low voltages are not isolated and additional care needs to be taken from the point of view of safety.

An example of a high-gain coupled inductor converter is shown in Figure 1.15 [15]. The converter consists of an active switch S, two diodes D_c and D_o. two capacitors C_c and C_o and the coupled inductors L_1 and L_2.

This converter and others of similar type [16]–[19] operate based on common principles: The diodes and switches are turned on and off in a complimentary manner during each switching period. Energy is stored in inductor L_1 when switch S is on and this energy is then transferred to the output when the switch is subsequently switched off. When the switch is turned off, a voltage is induced across the inductor L_2 and this is added to the voltage across L_1 and this mechanism brings in the extra voltage gain seen in this boost converter topology. Capacitor C_c is used to clamp the active switch voltage when its turned off.

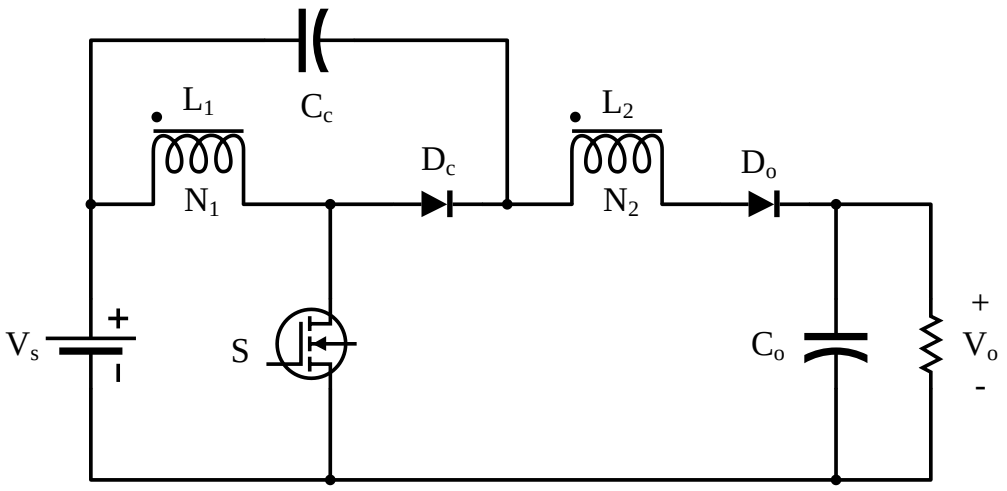

Figure 1.15: Schematic of a coupled inductor boost converter [15]

As the inductors are coupled,

$$n = \frac{n_2}{n_1} \tag{1.3}$$

where n_1 is the number of turns in inductor L_1 and n_2 is the number of turns in inductor L_2. The voltage gain equation of this coupled inductor boost converter can be determined to be

$$\frac{V_{out}}{V_{in}} = \frac{1 + nD}{1 - D} \tag{1.4}$$

From equation 1.4, it can be seen that the gain is more than a conventional boost converter and it can be further increased by changing the turns ratio n.

1.3.1.4 Flyback boost converter with voltage multiplier

Another way to increase voltage gain is by stacking output voltage in a voltage multiplier arrangement as shown in Figure 1.16. In this topology, and others of similar type [20]–[23], a flyback converter mechanism is used to produce a stepped up output voltage using a coupled inductor/transformer and this output is stacked on top of a boost converter output. In the converter shown in Figure 1.16, a square-wave AC voltage appears across L_1 and this AC voltage is stepped up by the coupled inductor so that a higher AC voltage appears

across L_2. This voltage is then rectified by diodes D_{o2} and D_{o3} so that DC voltage appears across C_{o2} and C_{o3}. The output voltage is the sum of the voltage across all three capacitors. The voltage gain can be expressed as

$$\frac{V_{out}}{V_{in}} = \frac{1+n}{1-D} \tag{1.5}$$

As with the coupled inductor converters discussed in the previous section, the main drawback of this type of converter is the lack of isolation between low input side voltages and high output side voltages.

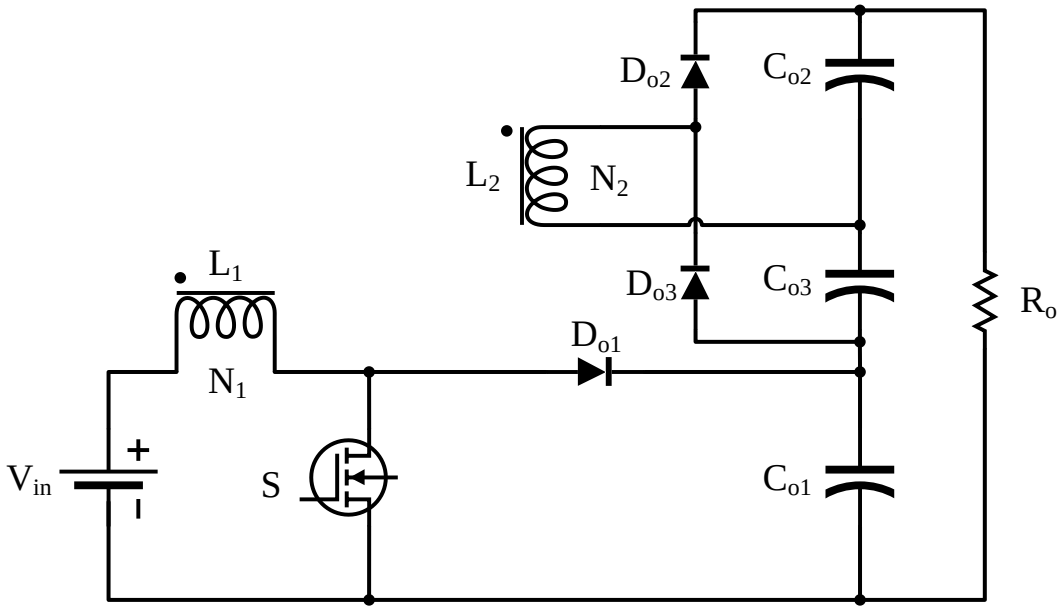

Figure 1.16: Flyback boost converter with voltage multiplier [23]

1.3.2 Passive snubbers

The second concept that will be used in the development of a new high-gain DC-DC converter is that of snubbers. Snubbers [24]–[28] are small networks of electrical components in power converters whose main purpose is either to clamp voltage spikes that can occur whenever a switch is turned off or current spikes that can occur when a switch is turned on. Snubbers may be either passive or active networks. Passive snubber network elements are limited to resistors, capacitors, inductors and diodes. Active snubbers include

transistors and other active elements and are thus more complex and more expensive. As the proposed converter will be implemented with a novel passive snubber arrangement, this section will focus on passive snubbers.

Voltage spikes can be caused by the interaction of converter parasitic inductance due to wiring or printed circuit board (PCB) tracks and the output capacitance of a MOSFET switch – when a switch is turned off, the energy trapped in parasitic inductance can be transferred to the output capacitance of the switch so that a voltage spike that exceeds the peak rating of the switch can be created. Such a spike can cause the switch device to be damaged. A capacitor placed in parallel with the switch will limit the voltage across those it. Current spikes can be caused by the turning on a switch – when a switch is turned on, the rise in current can be very sudden and some means are required to limit this rise, which can cause high current spikes to appear. An inductor placed in series with a switch will limit any rise in current when it is turned on. Examples of conventional voltage and current snubber circuitry is shown in Figure 1.17.

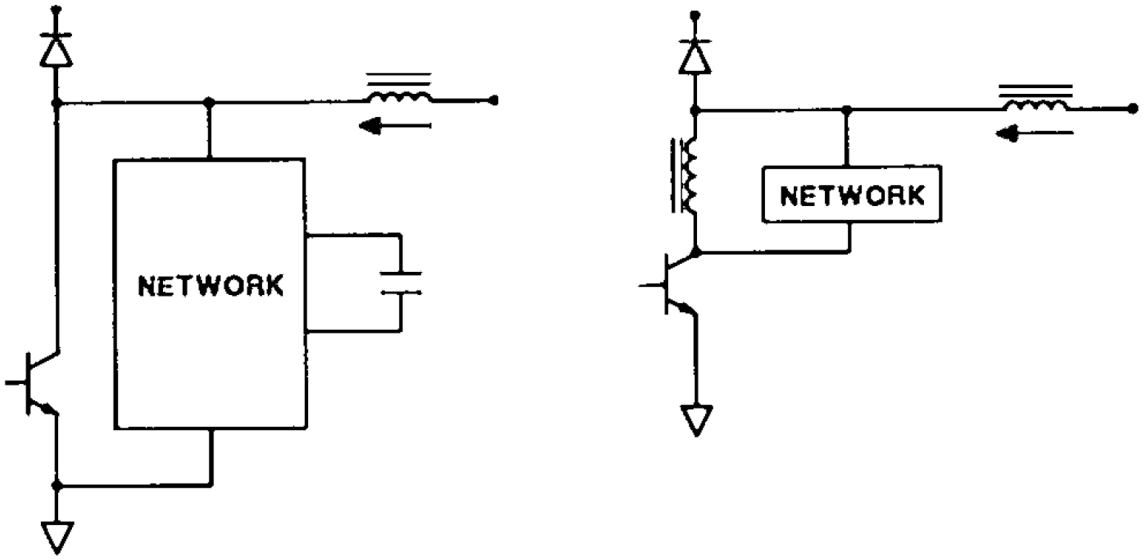

Figure 1.17: Voltage and current snubber circuits [28]

1.3.3 Z-source converter topologies

The third concept that will be used in the development of a new high-gain DC-DC converter is that of Z-source converter topologies [29]–[35]. A Z-source converter is

inherently different from conventional voltage or current source converters. The distinguishing feature is the inclusion of inductors, capacitors, and diodes in the input side and its introduced to step up or step down voltage. The amount of stepping up or stepping down is related to how often the converter is allowed to enter a shoot-through mode of operation. Since such a mode is similar to the shoot-through mode of a current-fed converter that causes voltage in this type of converter to be stepped up, the higher the frequency of such shoot-through modes in a Z-source converter, the higher the output voltage will become.

Figure 1.18 shows the generalised topology of the Z-source converter. It shows a network consisting of inductors L_1 and L_2 and capacitors C_1 and C_2 connected in an X shape which together forms the impedance source coupling the converter to the source. In voltage source converters, the upper and lower devices of each leg cannot be switched on simultaneously on purpose or switch misfiring; otherwise, a shoot-through would occur and destroy the devices. The shoot-through problem caused by misfiring is the major threat to converter's reliability [36]–[38]. In current source converters, however, at least one of the upper devices and one of the lower devices have to switched on and maintained on at any time; otherwise, an open circuit problem arises and this is a threat to this converter's reliability.

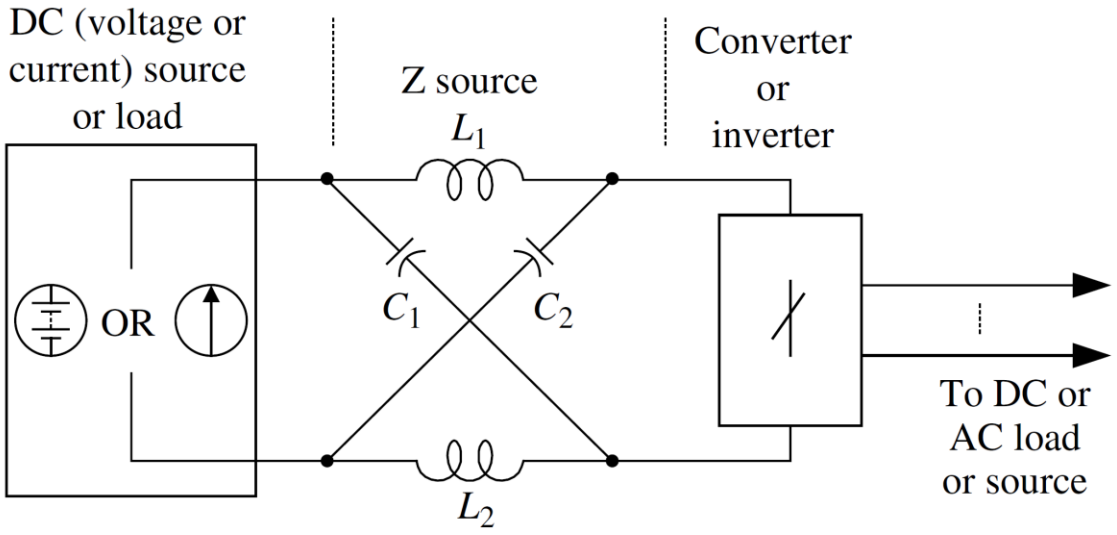

Figure 1.18: General topology of Z-source converters [29]

With the Z-source converter shown in Figure 1.18, if there is no switch on in the converter, current will flow through the capacitors in the passive network; if there is a shoot-through path in the converter, the presence of L_1 and L_2 will limit the rise in current. In essence, the passive element network of a Z-source converter is similar to a passive snubber as was described in the previous section. The main difference is that while a passive snubber is designed to operate for only a small fraction of a switching cycle, whenever a switch is turned on or off, the passive element network of a Z-source converter is designed to operate throughout the switching cycle.

1.4 Thesis objectives

The main objectives of this thesis are as follows:

1. To propose a novel DC/DC full bridge boost converter with high voltage gain, galvanic isolation between the source and load, simple PWM operation, fault ride through capability and ability to scale for higher power applications.

2. To analyze its steady state operation and to determine its steady state characteristics using circuit analysis techniques.

3. To develop design guidelines and a procedure to design the components of the topology to ensure the proper operation of the new converter.

4. To confirm the feasibility of the proposed power converter with results obtained from a working experimental prototype.

5. To draw conclusions from the work carried out and to suggest improvements to the converter.

A systematic approach was undertaken to achieve the objectives listed above and will be elaborated in the chapters to come in the order listed.

1.5 Thesis outline

The remainder of this thesis is comprised of the following chapters:

Chapter 2: The proposed high gain DC-DC full bridge converter is introduced in this chapter and its topology and operation are discussed. The modes of operation that the converter goes through are explained in detail. The attractive features of the new converter are stated in this chapter as well.

Chapter 3: A steady state analysis of the proposed converter is performed in this chapter. The purpose of the analysis is to derive expressions and determine relations of key converter parameters to understand the steady state characteristics of the converter. This process is required to establish a procure for the converter design that will be carried out in the following chapter.

Chapter 4: The design of the converter is discussed in this chapter. Design considerations are outlined and design guidelines are developed based on analysis carried out in Chapter 3. These guidelines and the overall design process are used to design a working prototype of the converter. The experimental results from the prototype converter will confirm the feasibility of the converter.

Chapter 5: In this chapter, the contents of the thesis are summarized. Conclusions are drawn from the work described in this thesis, and the main contributions are highlighted. The chapter concludes by suggesting potential future research work that can be carried out based on the thesis work.

Chapter 2

2 A new high gain DC-DC full bridge converter

In this chapter, the proposed high gain DC-DC full bridge converter is introduced and its topology and operation are explained. The various modes of operation that the converter goes through are explained in detail, and the attractive features of the new converter are highlighted and described.

2.1 Circuit description

A new high gain power converter that can be used for applications requiring very high voltage gains is proposed in this thesis. The proposed converter, shown in Figure 2.1, consists of a four-switch full-bridge, S_1, S_2, S_3 and S_4, an input inductor L, a power transformer T_3, secondary diodes D_2 and D_3 and an output capacitor C_{o2}. These components constitute the main part of the converter circuit. The converter also has a passive element network that consists of capacitors C_1 and C_2, transformers T_1 and T_2, and diode D_z. This passive circuit network is the same as that of the Z- source converter shown in Figure 1.18 except that the inductors have been replaced by transformers; the network also acts as a snubber to clamp voltage spikes that may otherwise be created whenever a switch is turned off. This passive snubber network is then advantageously used to increase the over all gain of the proposed topology.

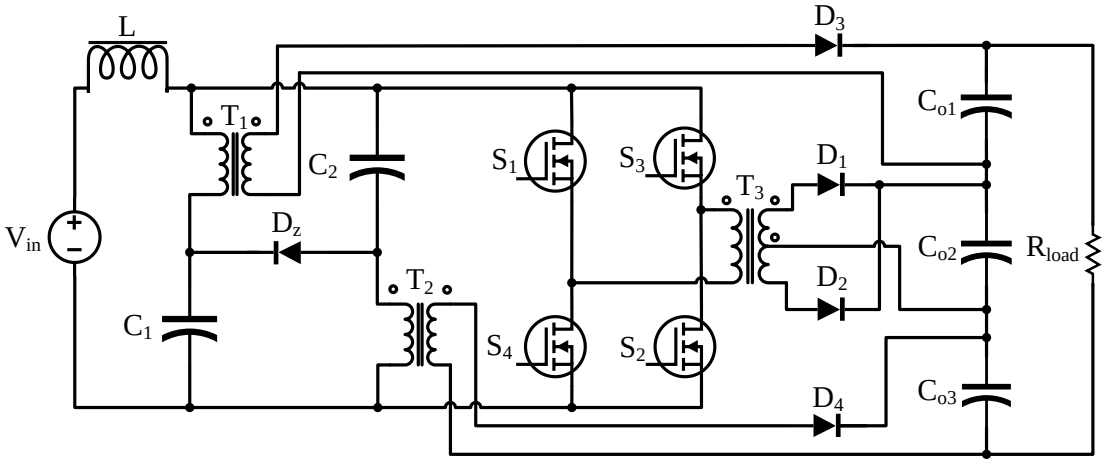

Figure 2.1: Proposed high-gain DC-DC converter

Diodes D_1 and D_4 are the secondary diodes for transformers T_1 and T_3 respectively and capacitors C_{o1} and C_{o3} are the secondary output capacitors for the two auxiliary snubber circuit transformers.

Transformers T_1 and T_2 allow a path for energy to be transferred to the output. If the secondary winding of these two converters are stacked on top of the output capacitor of the main circuit, then the voltage gain of the resultant converter can become greater than the circuits described in the literature review earlier.

The novel snubber network can be realized with minimal increase in the converter's cost as the additional components are generally passive components which don't need their own gate drivers or complicated control circuitry.

2.2 Converter operation

The proposed converter shown in Figure 2.1 is essentially a boost converter, but with transformer isolation and a DC bus snubber. When the input inductor is operating with continuous current, the main power circuit has two basic modes like a boost converter – one mode where the DC bus is shorted, another when energy is transferred to the output. The snubber circuit has other modes that will be explained later in the thesis.

The short-circuit mode occurs whenever two switches of the same bridge leg are on at the same time. This can occur with one converter leg or with both converter legs, when all the converter switches are on at the same time. When the switches of both legs are on, current can be distributed between the two legs, thus reducing peak current switch stresses.

The energy transfer mode occurs when a diagonally opposed pair of switches is on, either S_1 and S_2 or S_3 and S_4. When this happens, current flows through the primary winding of the main power transformer T_3.

While this sequence of short-circuit and energy transfer modes is occurring, the input inductor current rises when the converter is in a short-circuit mode and falls when it is in an energy transfer mode. This is a crucial mechanism intrinsic to boost converters and is required to operate the converter in steady state.

The basic sequence that the main power circuit goes through during a switching cycle is as follows: short-circuit → energy transfer → short-circuit → energy transfer, thus corresponding to that of a conventional single-switch boost converter. For example, this sequence can be seen in Figure 2.2, where the sequence shown is (S_1, S_2, S_3, S_4) → (S_3, S_4) → (S_1, S_2, S_3, S_4) → (S_1, S_2).

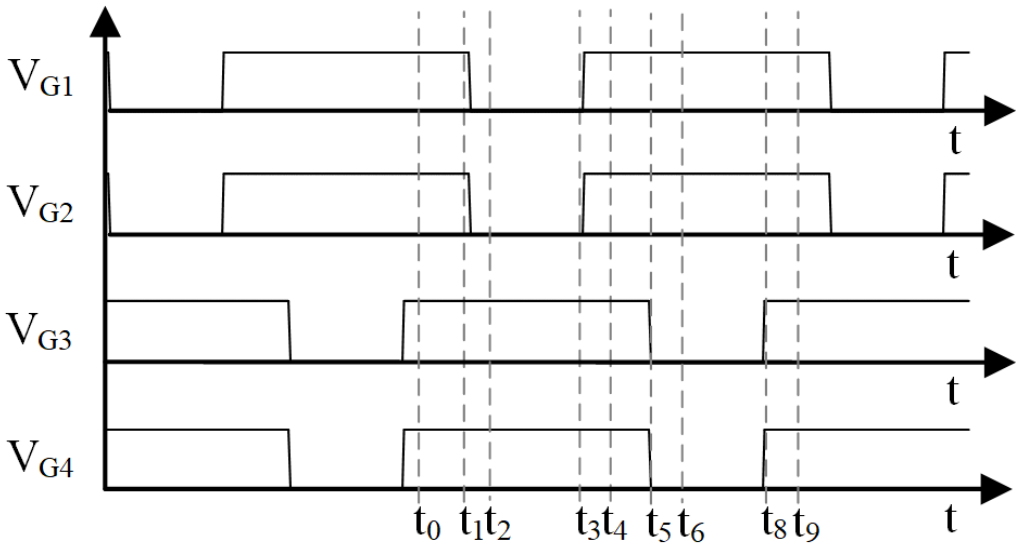

Figure 2.2: Typical converter gating signals

The modes of operation that the proposed converter goes through during a half switching cycle and their corresponding circuit diagrams are shown below. The modes of one half-cycle (t_0 to t_4) are identical to those of the other half-cycle (t_4 to t_5) except that a different diagonal pair of switches is on. The modes are as follows:

2.2.1 Mode 1 ($t_0 < t < t_1$)

All four converter switches (S_1, S_2, S_3 and S_4) are on at the start of this mode. The input current rises as the full input voltage is impressed across the input inductor L. No energy is transferred to the output from the auxiliary circuit or through the main power transformer. Instead, energy from the source is stored in the input inductor and hence this mode is a crucial mode and is found in all boost converter topologies.

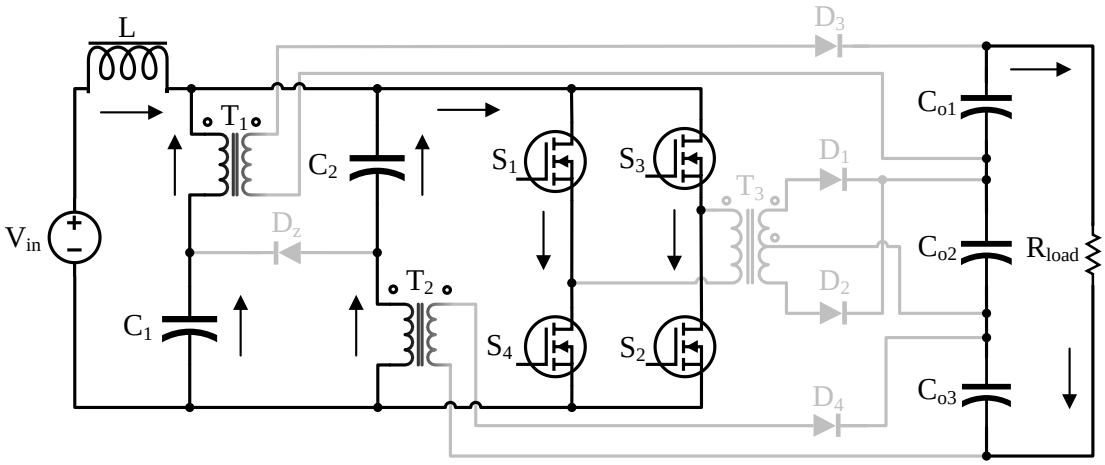

Figure 2.3: Mode 1 ($t_0 < t < t_1$)

2.2.2 Mode 2 ($t_1 < t < t_2$)

Switches S_1 and S_2 are turned off at the start of this mode. The converter transitions from a short-circuit mode to an energy-transfer mode during this mode, which is of short duration. While this is happening, energy begins to be transferred to the output through all three converter transformers. Current in the auxiliary snubber circuit capacitors C_1 and C_2 reverses direction and diode D_z conducts current. The primary current in the auxiliary transformers is gradually decreasing during this mode and the input current begins to decrease as well.

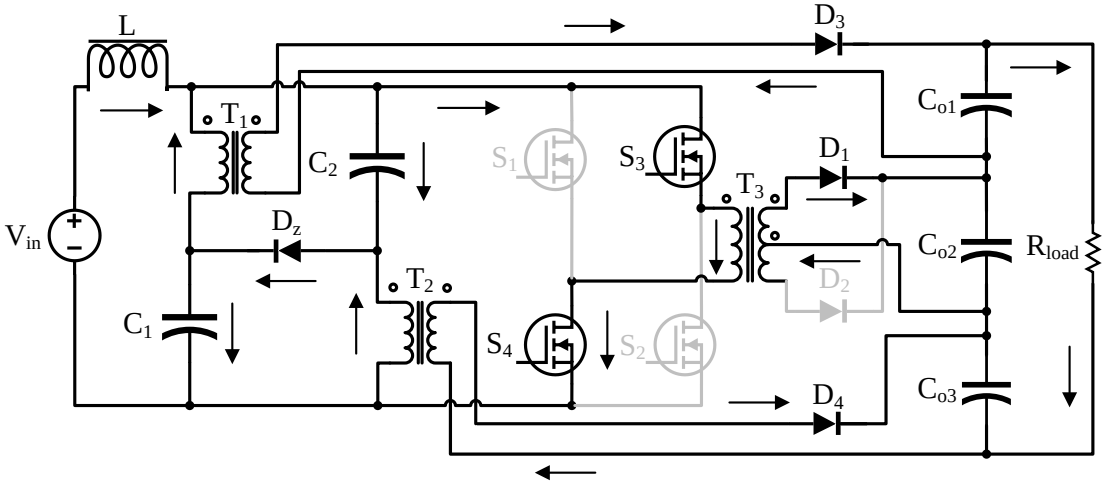

Figure 2.4: Mode 2 ($t_1 < t < t_2$)

2.2.3 Mode 3 ($t_2 < t < t_3$)

This mode begins when auxiliary circuit diode D_z stops conducting and the currents in capacitors C_1 and C_2 and the primary of the two auxiliary circuit transformers are the same.

The input current continues to fall and energy continues to be transferred to the output during this mode. The converter remains in this mode until switches S_1 and S_2 are turned on.

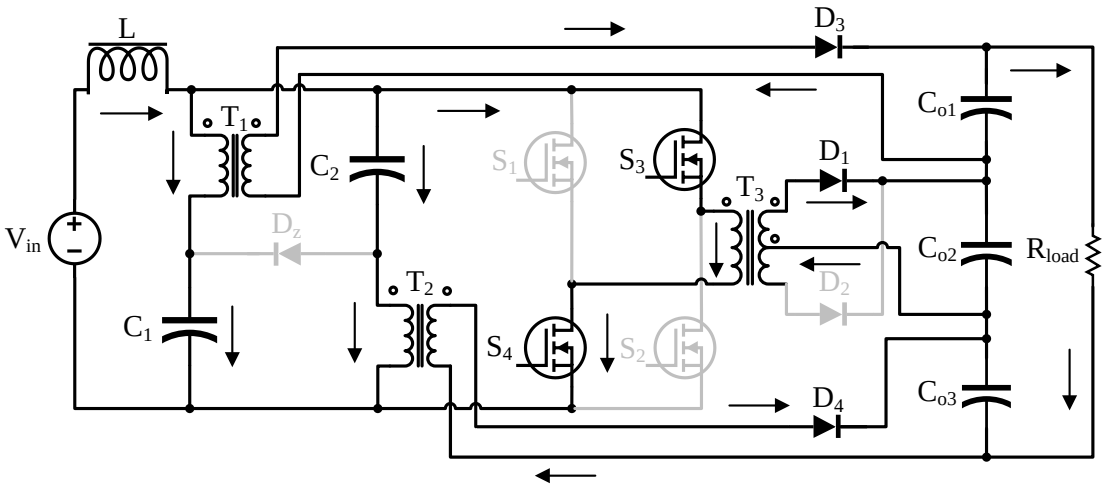

Figure 2.5: Mode 3 ($t_2 < t < t_3$)

2.2.4 Mode 4 ($t_3 < t < t_4$)

Switches S_1 and S_2 are turned on at the start of this mode. This mode is a transition mode of short duration as the converter is transitioning to a short-circuit mode.

During this mode, the currents in the secondary diodes of all the transformers begin to fall while the input current starts to rise. The primary current in the auxiliary transformers begins to decrease as well.

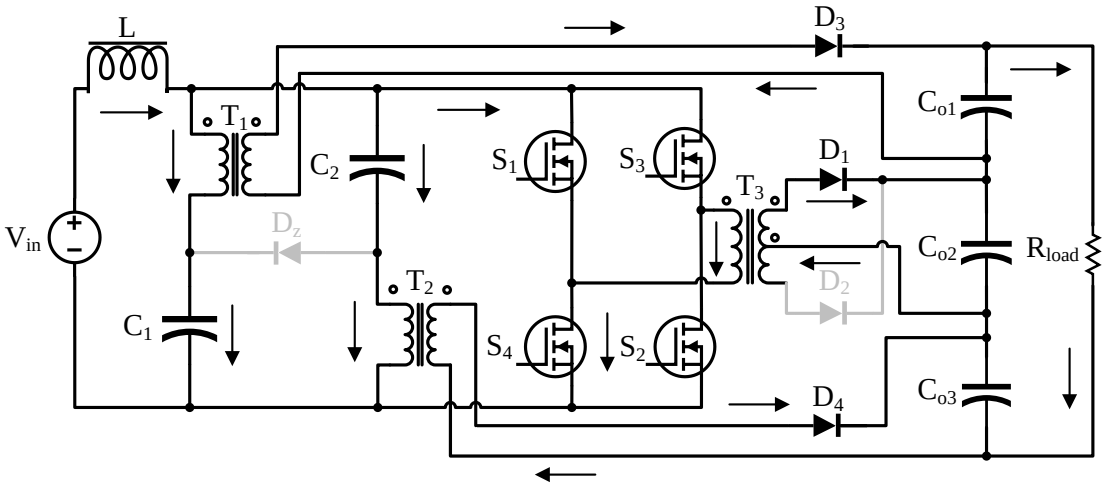

Figure 2.6: Mode 4 ($t_3 < t < t_4$)

2.2.5 Mode 5 ($t_4 < t < t_5$)

All four converter switches (S_1, S_2, S_3 and S_4) are on at the start of this mode. The input current rises as the full input voltage is impressed across the input inductor L.

No energy is transferred to the output from the auxiliary circuit or through the main power transformer. Instead, energy from the source is stored in the input inductor.

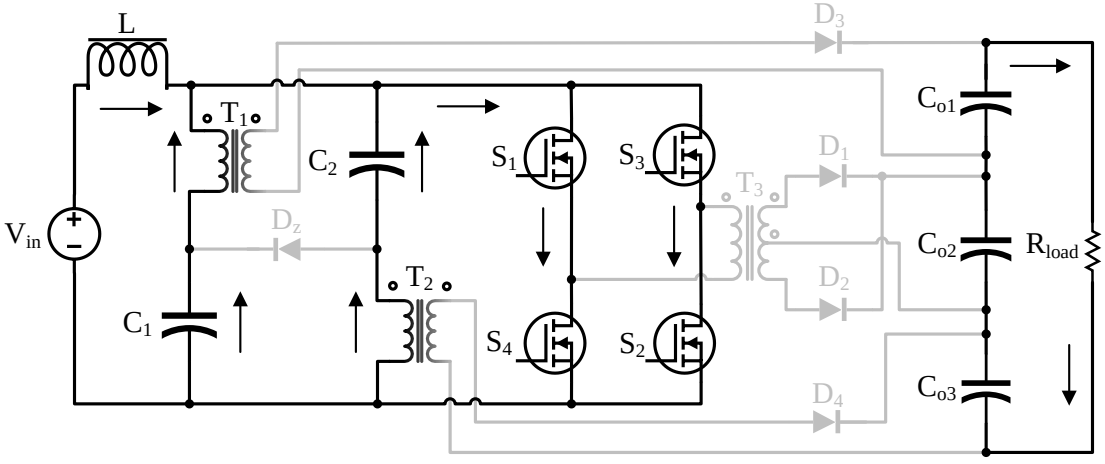

Figure 2.7: Mode 5 ($t_4 < t < t_5$)

2.2.6 Mode 6 ($t_5 < t < t_6$)

Switches S_3 and S_4 are turned off at the start of this mode. The converter transitions from a short-circuit mode to an energy-transfer mode during this mode, which is of short duration.

While this is happening, energy begins to be transferred to the output through all three converter transformers. Current in the auxiliary snubber circuit capacitors C_1 and C_2 reverses direction and diode D_z conducts current. The primary current in the auxiliary transformers is gradually decreasing during this mode and the input current begins to decrease as well.

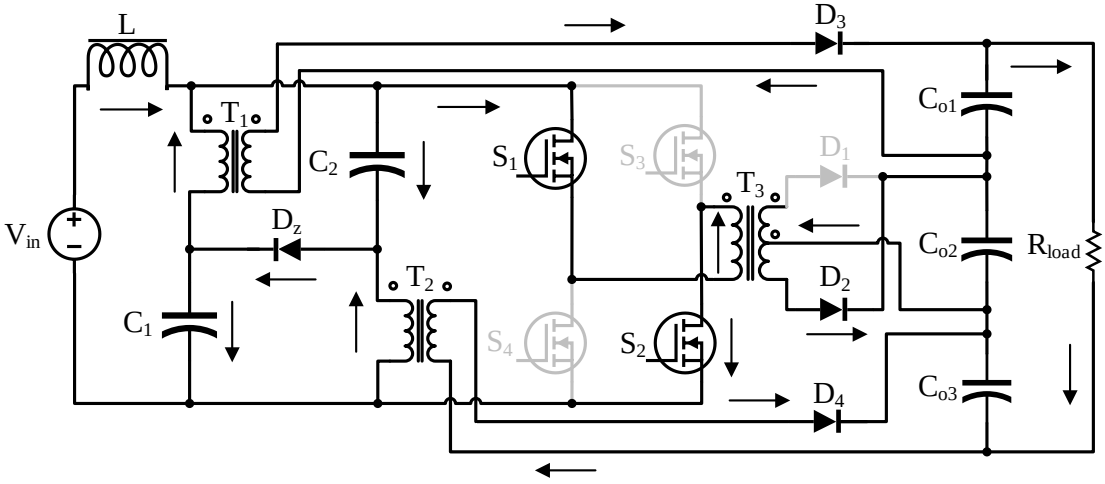

Figure 2.8: Mode 6 ($t_5 < t < t_6$)

2.2.7 Mode 7 ($t_6 < t < t_7$)

This mode begins when auxiliary circuit diode D_z stops conducting and the currents in capacitors C_1 and C_2 and the primary of the two auxiliary circuit transformers are the same. The input current continues to fall and energy continues to be transferred to the output during this mode.

The converter remains in this mode until switches S_3 and S_4 are turned on.

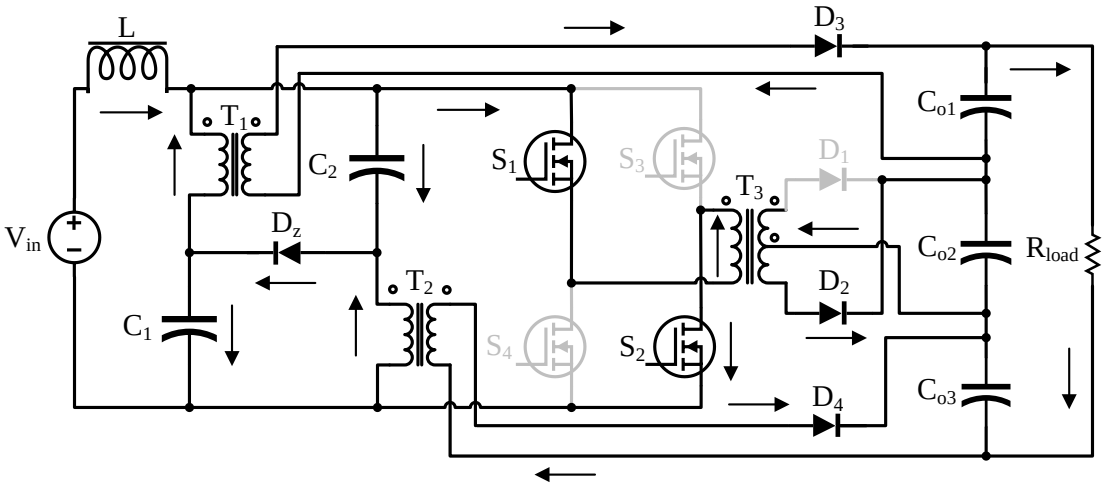

Figure 2.9: Mode 7 ($t_6 < t < t_7$)

2.2.8 Mode 8 ($t_7 < t < t_8$)

Switches S_3 and S_4 are turned on at the start of this mode. This mode is a transition mode of short duration as the converter is transitioning to a short-circuit mode.

During this mode, the currents in the secondary diodes of all the transformers begin to fall while the input current starts to rise. The primary current in the auxiliary transformers begins to decrease as well. The converter enters Mode 1 to start a new switching cycle by the end of this mode.

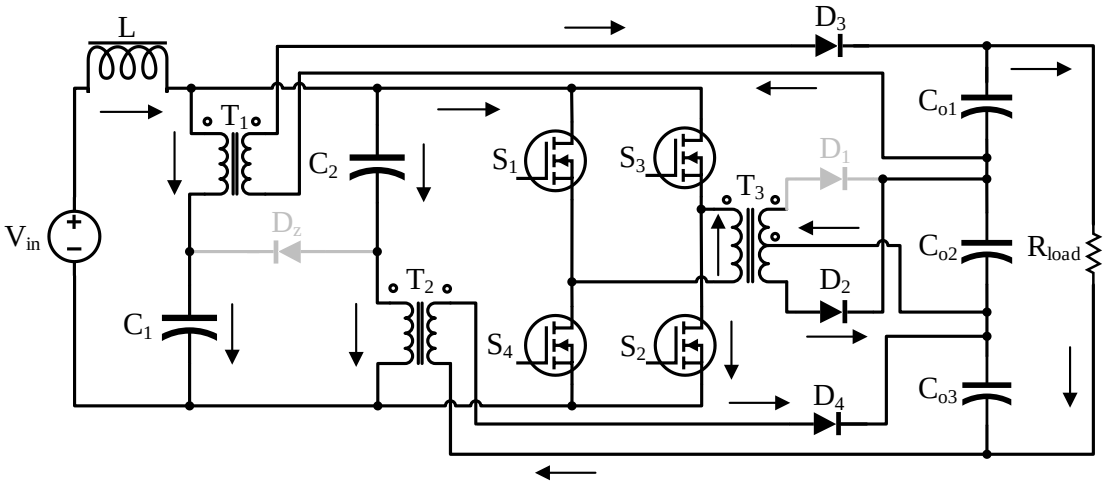

Figure 2.10: Mode 8 ($t_7 < t < t_8$)

The detailed modes of operation were described above and serve as an important tool to both understand the circuit and to derive the equations in the next chapter. Typical waveforms of the converter are shown below in Figure 2.11 and aim to further illustrate the operation modes of the converter.

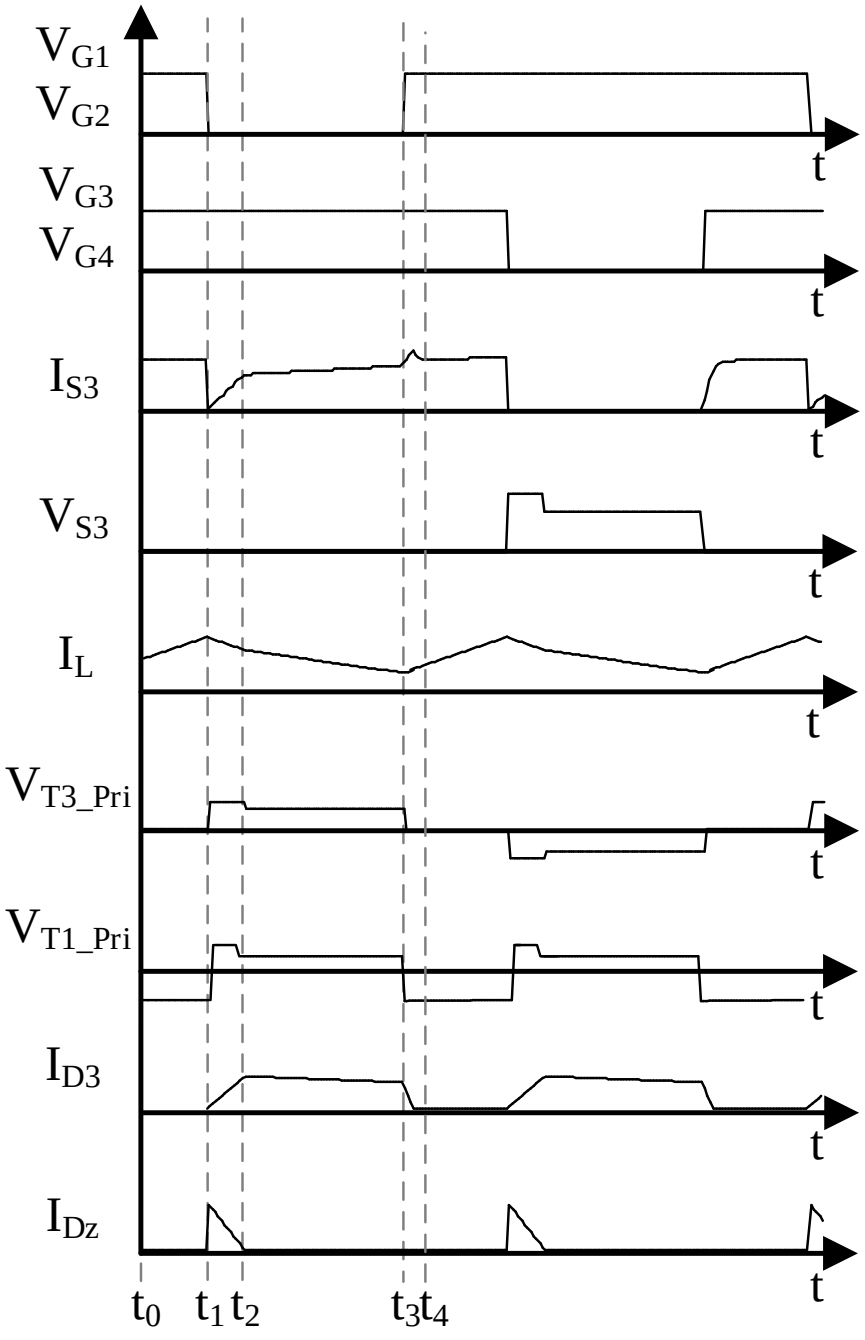

Figure 2.11: Converter waveforms

2.3 Converter features

The proposed converter has the following features:

- Since energy from the snubber circuit can be transferred to the output instead of just circulating in the primary side, the converter can have a high voltage gain. The energy stored in the snubber capacitors is not dissipated through a resistor or a switch, as is the case with many passive snubbers. The energy is transferred to the output instead.

- The converter's DC bus auxiliary circuit acts as a snubber that can clamp voltage spikes that would otherwise occur when the converter was turned off.

- The converter operates with standard PWM control and can be implemented with any commercially available PWM control IC.

- There is galvanic isolation between the low-side voltage and the high-side voltage. This isolation increases reliability and allows the use of this converter for applications where an isolated load needs to be driven.

- The converter is "open-circuit proof" as there is a path for current to flow through the auxiliary circuit if the converter switches somehow misfire and there is no available path for current to flow through. Current can flow through auxiliary circuit capacitors C_1 and C_2 and diode D_z until the converter switches return to normal operation. This increase the over all fault ride through capability of this converter

- The input current is continuous i.e. it is not chopped up during the switching cycle like other switched mode power supplies. This allows interfacing sensitive sources such as batteries without additional input side filters.

- Since the input current is continuous, the semiconductor peak current stresses are not excessive. The peak voltage and current stressed are comparable to other current fed full bridge DC-DC converters.

2.4 Conclusion

This chapter serves as an introduction to the novel high gain DC-DC converter topology proposed in this thesis. The modes of operation of this converter were described in detail along with circuit diagrams and waveforms to illustrate its operation. The features of this converter were highlighted and stated. The modes of operation described in this chapter will be used to derive the equivalent modes for steady state analysis in the next chapter.

Chapter 3

3 Converter analysis

A steady-state circuit analysis of the proposed converter is carried out in this chapter followed by simulations of the topology using a commercially available circuit simulator. Steady-state in this case refers to an operating state of the converter where the voltages and currents of the components at the end of the switching cycle are equal to the values at the start of the cycle.

Steady state analysis serves as an important tool to derive expressions and relations of key converter parameters to understand, and define the steady state characteristics of the converter. The simulations serve as preliminary verification of these derived equations and also serve as an aide to visualize the converter waveforms. This analysis then serves as the foundation on which the design guidelines outlined in chapter four are based on.

3.1 Steady state circuit analysis

The initial analysis used to establish the steady state operating points is based on the following assumptions:

- The converter is in steady state
- The switching period is T, all the switches are closed for time D_sT and one of the two switch pairs (S_1 and S_2 or S_3 and S_4) are open for $(1-D_s)$ T.
- The converter operates in continuous conduction mode i.e. the inductor current is continuous or positive.
- The output voltage is held constant by a fixed load.
- The components are ideal

With these assumptions in place, the equivalent circuits for the important modes of operation are drawn and the voltage and currents are defined. This is then used to obtain a

voltage gain relationship which is then used to derive the passive component equations followed by the voltage and current stress for active and passive devices.

3.1.1 Equivalent circuits for significant modes of operation

The equivalent circuits of the converter's important modes of operation are shown below along with the equations associated with that mode. The transition modes are not included and the passive components are assumed to be charged.

The figure below shows the proposed converter's equivalent circuit in the active operation mode when one of the switch pairs either S_1 and S_2 or S_3 and S_4 are switched on and power flows to the load.

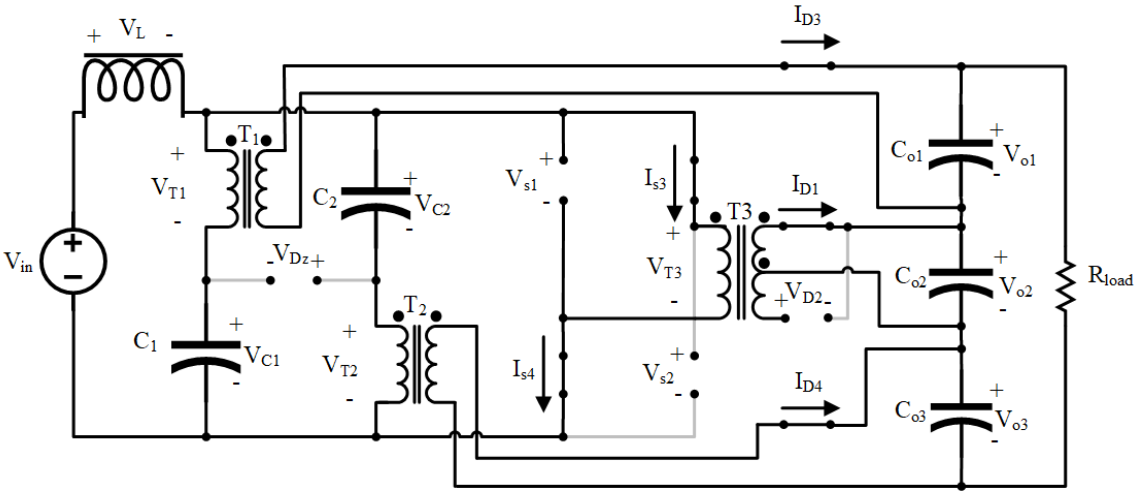

Figure 3.1: Equivalent modes for active mode

The following set of equations can be written for this operation mode:

$$V_{ox} = nV_{Tx} \tag{3.1}$$

Equation 3.1 shows the output voltages based on transformer turns ratio as seen from output side and where x is either 1, 2 or 3.

$$V_L = V_{in} - V_{T3} \tag{3.2}$$

$$V_L = V_{in} - \frac{V_{o2}}{n} \tag{3.3}$$

$$V_{T1} = V_{T3} - V_{C1} \tag{3.4}$$

$$V_{o1} = V_{o2} - nV_{C1} \tag{3.5}$$

$$V_{T2} = V_{T3} - V_{C2} \tag{3.6}$$

$$V_{o3} = V_{o2} - nV_{C2} \tag{3.7}$$

$$V_{sx,max} = V_{T2} \tag{3.8}$$

Equations 3.2 to 3.7 show the inductor and transformer primary side voltages as seen from input side and are used in the next section to derive gain and duty ratio expressions

The figure below shows the equivalent circuit for the shoot through modes that the proposed converter goes through. This mode occurs when all the active switches are switched on.

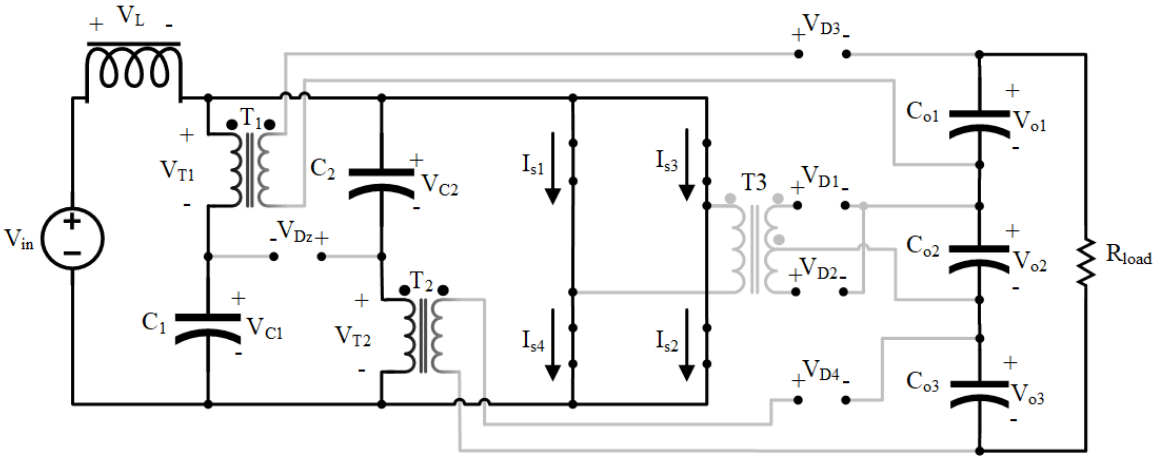

Figure 3.2: Equivalent circuit for shoot through mode

The following set of equations can be written for this operation mode:

$$V_L = V_{in} \tag{3.9}$$

$$V_{D3,max} = V_{co1} \tag{3.10}$$

$$V_{D1,max} = V_{D2,max} = V_{co2} \tag{3.11}$$

$$V_{D4,max} = V_{co3} \tag{3.12}$$

3.1.2 Voltage gain and duty cycle

The voltage gain equation for the main circuit is derived as follows: To maintain volt-second balance in the input inductor during steady-state operation, the voltage across the inductor should be zero over a period, according to

$$\langle V_L \rangle = \frac{1}{T}\int_0^t V_L(t)\, dt = 0 \tag{3.13}$$

From equations 3.3 and 3.9, we can obtain the voltage of the inductor during the shoot-through and active modes as follows:

$$\langle V_L \rangle = D_A\left(V_{in} - \frac{V_{o2}}{n}\right) + D_S(V_{in}) = 0 \tag{3.14}$$

It is known that

$$D_A + D_S = 1 \tag{3.15}$$

Substituting equation 3.15 in 3.14 and assuming D_s=D for simplicity

$$(1 - D)\left(V_{in} - \frac{V_{o2}}{n}\right) + D(V_{in}) = 0 \tag{3.16}$$

$$\frac{V_{o2}}{V_{in}} = n\left(\frac{1}{1 - D}\right) \tag{3.17}$$

This gives a relationship for the main circuit gain and is similar to that of the current-fed full bridge boost converter. Now using the methodology used for high gain topologies shown in the literature review [9]–[21], the gain of the whole converter can be derived according to

$$V_{out} = V_{o1} + V_{o2} + V_{o3} \tag{3.18}$$

Substituting voltages of the auxiliary circuit from equation 3.5 and 3.7 into 3.18 gives

$$V_{out} = V_{o2} - nV_{C2} + V_{o2} + V_{o2} - nV_{C1} \tag{3.19}$$

Since under steady-state conditions

$$V_{in} = V_{C1} = V_{C2} \tag{3.20}$$

therefore,

$$V_{out} = V_{o2} - nV_{in} + V_{o2} + V_{o2} - 2nV_{in} \tag{3.21}$$

Substituting the gain relationship of the main circuit from equation 3.17 into equation 3.21 gives

$$V_{out} = 3nV_{in}\left(\frac{1}{1-D}\right) - 2nV_{in} \tag{3.22}$$

$$\frac{V_{out}}{V_{in}} = n\left(\frac{1+2D}{1-D}\right) \tag{3.23}$$

The voltage gain, defined in equation 3.23 is plotted below for a turns ratio, n of one in Figure 3.3 below.

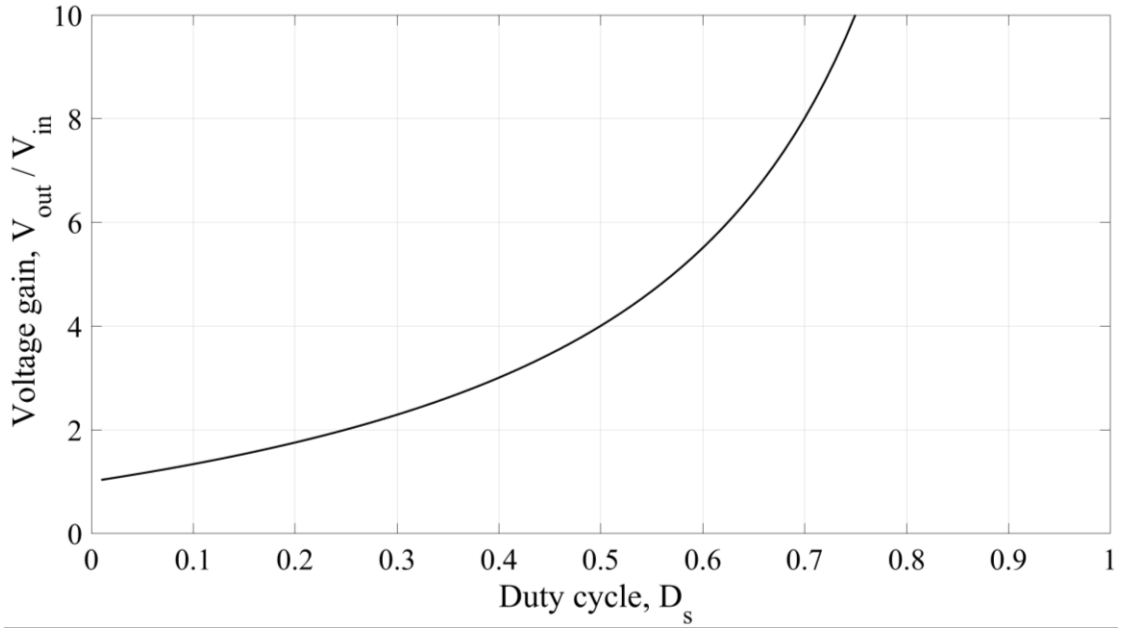

Figure 3.3: Proposed converter voltage gain vs. duty cycle

3.1.3 Critical inductance for CCM

Continuous conduction mode (CCM) is preferred for interfacing sensitive sources such as PV, fuel and lithium cells or batteries, i.e. the current through inductor is always positive in steady state as shown in the figure below.

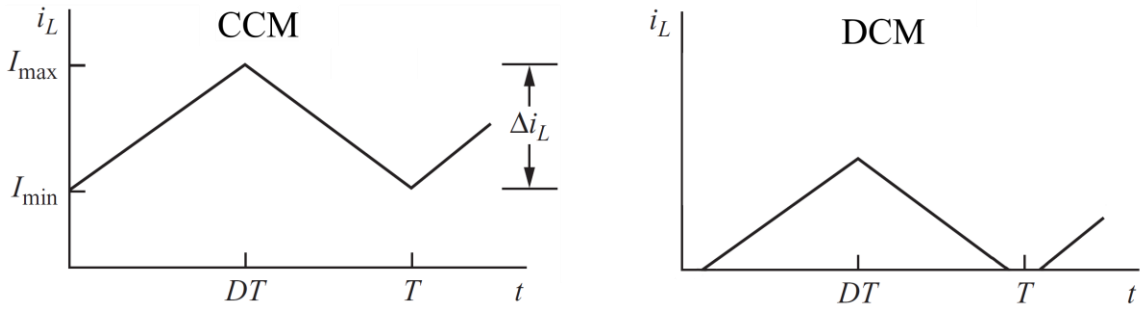

Figure 3.4: Continuous conduction mode vs. discontinuous conduction mode

To ensure CCM, the inductance of the input inductor has to be sufficiently large; a relationship is then derived in this section to define the critical point above which the converter operates in CCM.

A relationship between the input and output currents can be obtained by neglecting losses and equating input power and output power as follows:

$$V_{out} I_{out} = V_{in}\, I_{in} \tag{3.24}$$

$$V_{in} I_L = \frac{{V_{out}}^2}{R} = \frac{\left[n\left(\frac{1+2D}{1-D}\right) V_{in}\right]^2}{R} \tag{3.25}$$

$$I_L = \frac{n^2 \times \left(\frac{1+2D}{1-D}\right)^2 V_{in}}{R} \tag{3.26}$$

From Figure 3.4, the following relation for the minimum current can be obtained by considering the shape of the waveform:

$$I_{min} = I_L - \frac{\Delta i_L}{2} \tag{3.27}$$

The inductor value can be determined based on minimum current required to operate in continuous current mode. By setting $I_{min} > 0$, the following relation for the minimum inductance can be obtained:

$$I_{min} = \frac{n^2 \times \left(\frac{1+2D}{1-D}\right)^2 V_{in}}{R} - \frac{V_{in} T n}{2L_{min}} \left(\frac{1+2D}{1-D}\right) \tag{3.28}$$

$$L_{min} = \left(\frac{1-D}{1+2D}\right) \frac{R_{load}}{2nf} \tag{3.29}$$

3.1.4 Switch stress

Switches S_1, S_2, S_3, and S_4 experience voltage stresses based on the voltage impressed on them during the operation of an alternate pair of switches. From equations 3.8 and 3.17, the following equation, which represents the voltage stress seen by the switches, can be determined:

$$V_{sx,max} = V_{in} \left(\frac{1}{1-D}\right) \tag{3.30}$$

This value will be seen by the converter initially but as the auxiliary passive snubber network starts operating, the voltage will reduce. This is unlike the current-fed full-bridge converter where the switches see the maximum voltage stress during the whole duration as there is no auxiliary passive snubber.

3.2 PSIM simulation

The theoretical analysis and expressions are confirmed with a simulation study of the proposed converter in a commercially available power electronics simulation software, PSIM.

3.2.1 Simulation workspace

The proposed converter was simulated with the parameters shown in the table below to boost a voltage of 48V to 400V at 500W. The component values chosen for the simulation are as follows: input inductor, L is 400 µH for CCM operation, input capacitors, C_1 and C_2

are 10 µF, transformer turns ratio, n is 3, and the load resistance is 320 ohms. The other simulation parameters required for nodal analysis and control are shown in table 3-1 below.

Table 3-1: Simulation parameters

Frequency, f	50 kHz
Duty Cycle, D	0.38
Simulation time step	0.1 µs
Simulation time	0.5 s
Constant voltage, V_{in}	48 Volts

The voltage gain of the proposed converter from the simulation was

$$Gain_{simulation} = \frac{V_{out}}{V_{in}} = \left(\frac{400}{48}\right) = 8.\overline{3}$$

Based on equation 3.23, the voltage gain of the proposed converter in theory can be computed by substituting D=0.38 and n=3 which then gives

$$Gain_{theoretical} = n\left(\frac{1+2D}{1-D}\right) = 3\left(\frac{1+2\times 0.38}{1-0.38}\right) = 8.51$$

As can be seen from the simulated converter results and theoretical gain, the voltage ratio of the simulated converter is less than the theoretical gain. This discrepancy is due to the leakage inductance of the transformer as realistic leakage inductance was used in the simulations.

Waveforms from the simulations are shown below:

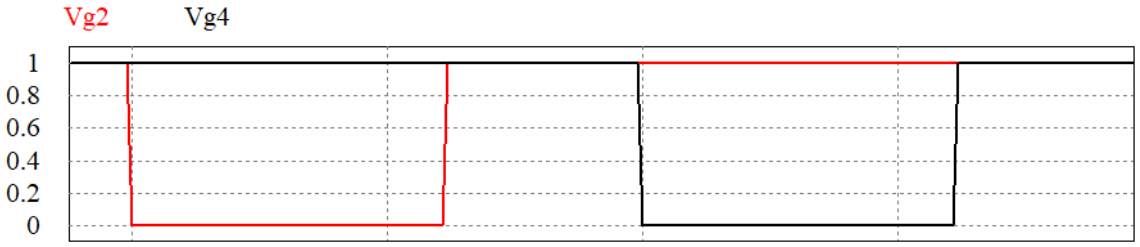

Figure 3.5: Gate pulses for a duty cycle of 0.38

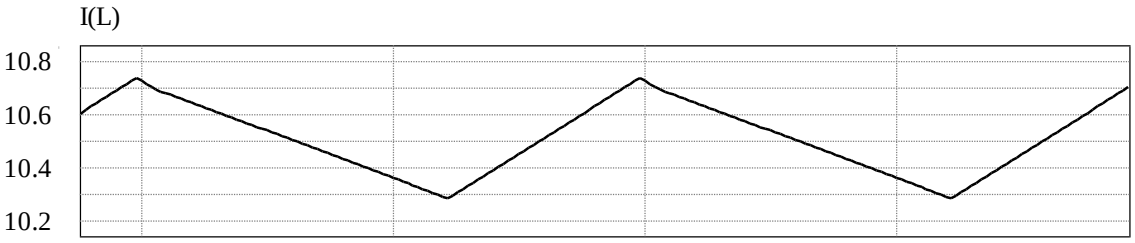

Figure 3.6: Inductor Current

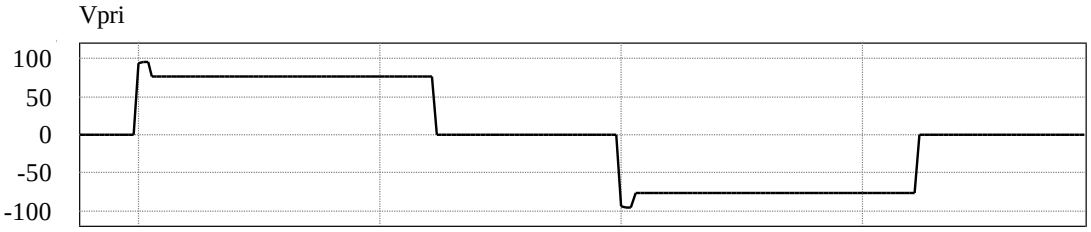

Figure 3.7: Voltage across main transformer

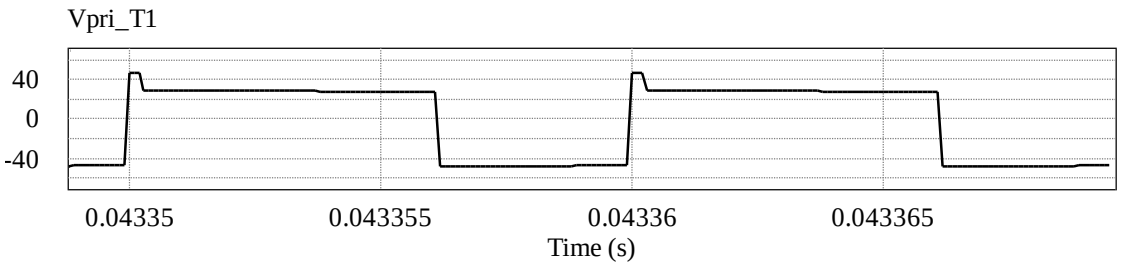

Figure 3.8: Voltage across auxiliary transformer

From Figure 3.6, it can be seen that the converter operates at continuous conduction mode using inductance values based on equation 3.29, which was derived to define the critical inductance point below which the converter would operate in discontinuous mode.

Figures 3.7 and 3.8 show the voltage across the main and auxiliary transformers, as can be seen there is a positive and negative voltage being applied it as per the volt second balance discussed earlier. This is crucial to ensure that the transformer does not saturate due to residual magnetism.

3.3 Conclusion

A steady state circuit analysis of the proposed converter was performed in this chapter. Expressions and relations for key converter parameters such as duty ratio, voltage gain, transformer turns ratio, critical input inductor values and switch stresses were determined and preliminary verification of the derived expressions was carried out using circuit simulators.

The purpose of the analysis was to understand the steady state characteristics of the converter and to dictate steady state operating points or regions. Insights and expressions derived in this chapter will be used to formulate a procedure for the proposed converter's design, which will be done in the next chapter of the thesis.

Chapter 4

4 Converter design

The design of the proposed converter is explained in this chapter. The design considerations and procedure are laid out based on the expressions derived in the steady-state analysis in the previous chapter. An example will be shown to demonstrate the process. Also, the results of the design process will be used in the implementation of a prototype converter that will be used to confirm the feasibility of the proposed converter topology.

4.1 Design considerations

For the design of the converter, the following parameters that are described in this section of the thesis must be considered:

4.1.1 Converter duty ratio, D

The duty cycle or duty ratio is an important criterion for converter design as the voltage gain of the converter before transformer turns ratio is dependant on this parameter. Duty cycle in this case and in general for a boost converter is the amount of time of time spent in shoot through modes compared to the total duration of a single cycle, according to

$$D = D_s = \frac{T_{shoot-through}}{T_{total}} \tag{4.1}$$

From the steady state circuit analysis carried out in Chapter 3, the following relation between output voltage V_{out}, input voltage V_{in} and the duty cycle D was determined:

$$\frac{V_{out}}{V_{in}} = n\left(\frac{1+2D}{1-D}\right) \tag{4.2}$$

From the theoretical expressions, values of D based on the required voltage gain and specifications of the converter can be obtained.

In reality, using a duty cycle of 0.2 to 0.7 is optimal to avoid the usual higher voltage and current stresses found in conventional boost converters at higher duty cycles[10].The duty

cycle is a crucial parameter for the gating pulses which drive the active switches, S_1 through S_4, as shown in Figure 4.1.

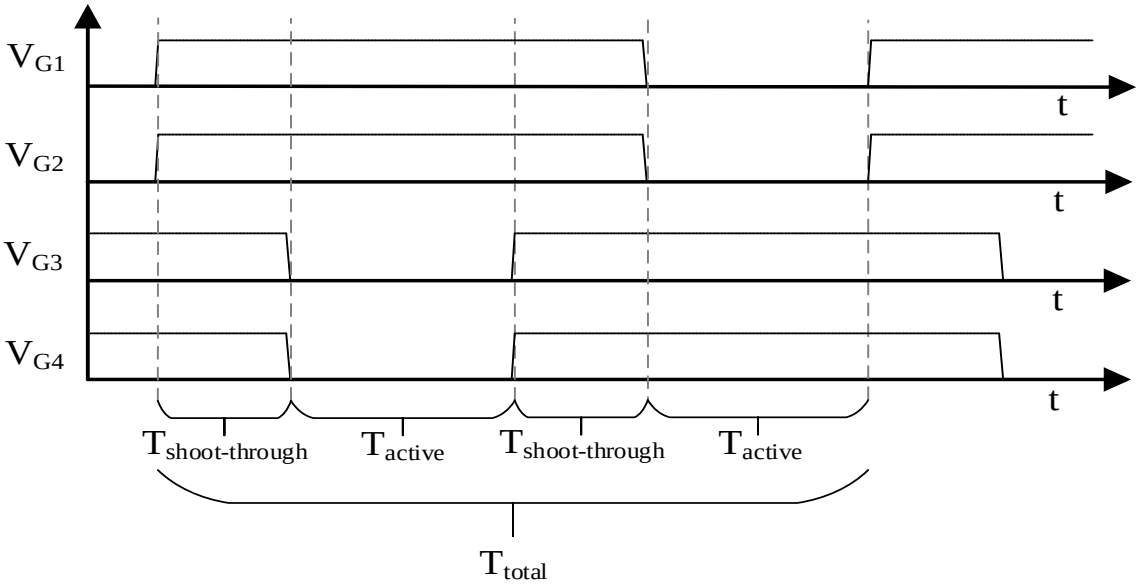

Figure 4.1: Gate pulses

4.1.2 Transformer turns ratio, n

In isolated power converters like the proposed converter topology, the transformer turns ratio is another important parameter that helps determine the required voltage gain. The inherent converter gain should be adjusted to be as high possible without excessive voltage or current stress, then the transformer turns ratio should be selected to obtain the rest of the voltage gain. This is done to reduce the current in the primary side of the converter. The same expression shown in equation 4.2 can be used to obtain the turns ratio, n, as required.

For simplicity, during the steady-state circuit analysis, the turns ratio of the main and auxiliary power transformers was assumed to be the same. The graph of voltage gain vs duty cycle for various values of n shown in Figure 4.2. can be used to select the turns ratio and duty cycle.

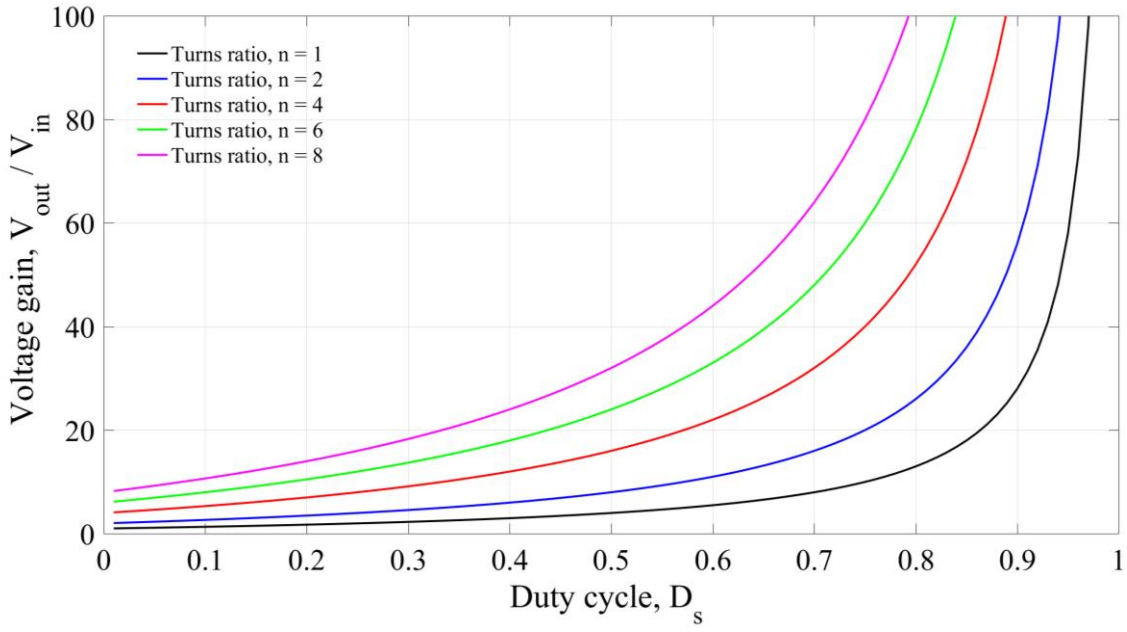

Figure 4.2: Voltage gain vs. duty cycle for different turns ratio

4.1.3 Input inductor rating, L

In boost converters operating in continuous conduction mode(CCM), a critical parameter to ensure that the converter operates in CCM is the inductance of the input inductor. The input inductor current of the proposed converter should be continuous to avoid high peak currents. The same is true for the design of the original converter as well as it is a low input voltage thus high input current converter. The inductance must be large enough to hold the current steady, that is it must be large enough to oppose a change in current. The minimum inductance to ensure this is

$$L_{min} = \left(\frac{1-D}{1+2D}\right)\frac{R_{load}}{2nf} \tag{4.3}$$

which was derived from steady-state circuit analysis performed in Chapter 3. This expression relates the minimum inductance L_{min} to the duty cycle D, equivalent resistance at maximum load R_{load}, turns ratio n, and frequency of the converter f.

The minimum inductance calculated using equation 4.3 is the value of the input inductor under DC bias and the overall magnetics design of the inductor is similar to boost

converters used in industry[39].In general the permeability of the ferrite core used to construct the inductor drops based on DC current bias and is shown in Figure 4.4

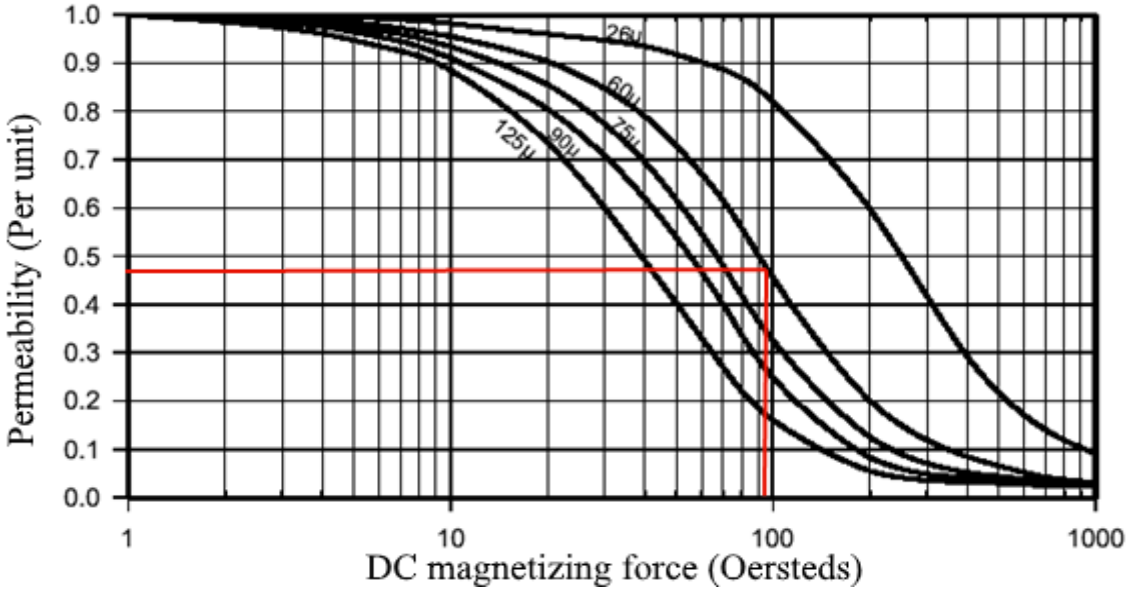

Figure 4.3: Effect of DC bias on permeability [39]

Therefore, the DC current is a crucial parameter. This current, $I_{L,avg}$ can be found using the following expression:.

$$I_{L,avg} = \frac{n^2 \times \left(\frac{1+2D}{1-D}\right)^2 V_{in}}{R} \tag{4.4}$$

which can be derived from equation 3.22 and 3.23.

4.1.4 Output and input capacitor rating, C_{ox}

The output capacitor rating affects the output voltage ripple and is generally specified in modern power supply standards. To conform to those standards, it must be ensured that the capacitance is large enough to curb the ripple that is inherent in a switching type converter.

For the proposed converter, a value for the output capacitor can be chosen by using the following equation, which is identical to that for the boost converter capacitor [10] except that it has been adjusted to take into account that the effective frequency seen by the output

is twice the converter switching frequency, given that there are two short-circuit modes and two energy transfer modes within a switching cycle:

$$C_{ox} = \frac{D}{2R_{load}\left(\frac{\Delta V_o}{V_o}\right)f} \tag{4.5}$$

Where V_o is the output voltage and ΔV_o is the peak to peak ripple.

As for auxiliary capacitor values, C_{o1} and C_{o3}, since the auxiliary circuit transformers can be considered to be parts of similar smaller power converters, the previous equation can be used with the lower voltage values that the auxiliary operates with equation 4.5 is suitable for its design as well.

4.1.5 Switch voltage stress, $V_{Sx,\,max}$

Switch voltage is another important parameter during a switched mode power supply design as the switches must tolerate high voltages during switching action and even with the passive snubber circuit in our proposed converter topology the maximum value is seen for some time until the auxiliary circuits kick in.

The following equation derived from equation 3.8 based on Figure 3.1 can be used to select the switches:

$$V_{Sx,max} = V_{in}\left(\frac{1}{1-D}\right) \tag{4.7}$$

4.1.6 Diode voltage stress, $V_{Dx,\,max}$

The selection of a appropriate device for the diode V_{Dx} is based on the maximum voltage seen across the various diodes in the circuit during the whole switching cycle as seen in Figure 3.2 and equation 3.10. This voltage can then be expressed as

$$V_{Dx,max} = V_{cox} \tag{4.8}$$

For the diodes in the output of the main center-tapped power transformer, the following equation based on equation 3.15 can be used, which describes the voltage seen by the secondary side:

$$V_{Dx,max} = nV_{in}\left(\frac{1}{1-D}\right) \tag{4.9}$$

The auxiliary circuit diode voltages can be determined using the following equation, which similarly is based on the voltage seen at the secondary of the auxiliary transformers:

$$V_{Dx,max} = nV_{in}\left(\frac{1}{1-D}\right) - nV_{in} \tag{4.10}$$

The input side diode, D_z sees the input voltage during steady state operation.

4.2 Design procedure

The design of the proposed converter is an iterative process as many of the key converter parameters described above are related to one another. This section describes a sequential process that can be used to formulate the converter design for a given set of specifications, using the expressions and graphs shown in this section. First, the specifications are to be assessed. The required input and output voltage range along with the maximum power that the converter is to operate safely is crucial for the design process. Once the operating range of the input voltage is known, the converter can be designed to provide a fixed output voltage and maximum power rating. This can be done by choosing an operating region in Figure 4.2 which illustrates voltage gain vs duty cycle, this figure can be used to tweak the duty cycle to account for input voltage variances. This data is then used to create a controller that will change the duty cycle as required to maintain a constant output voltage.

After choosing the steady-state operating region, component ratings based on key parameters mentioned earlier can be determined. Key passive components like inductors and capacitors are to be selected based on expressions and figures discussed earlier. Active components are to be selected based on voltage and current stresses along with the desired switching frequency and power.

4.3 Design example

To verify the feasibility of the converter, a prototype with the following specification is to be designed.

Table 4-1: Example specifications

Input voltage, V_{in}	48 Volts
Output voltage, V_{out}	400 Volts
Power, P	250 Watt
Ideal switching frequency, f	50 kHz

In this example, a voltage gain of ~8.3 is required; equation 4.1 and Figure 4.2 can be used to obtain the operating region as follows:

$$\frac{400}{48} = n\left(\frac{1+2D}{1-D}\right) \tag{4.11}$$

A transformer turns ratio, n of 3.5 can be chosen based on Figure 4.2. A lower duty cycle can then be chosen to both highlight the higher boost ratio and to account for practical duty cycle limitations due to slew rate limitations, feedback compensation stability and the need to avoid any negative parasitic effects.[40]–[42]

Substituting this in equation 4.11 gives

$$\frac{400}{48} = 3.5\left(\frac{1+2D}{1-D}\right)$$

From this equation, a duty cycle of ~0.31 can be obtained for our input voltage, V_{in} = 48 volts.

The critical inductance for CCM operation can be determined from equation 4.3 and is based on the load resistance and switching frequency.

$$L_{min} = \left(\frac{1 - 0.31}{1 + 2 \times 0.31}\right)\frac{R_{load}}{2 \times 3.5 \times 50 \times 10^3} \quad (4.12)$$

R_{load} can be calculated based on required power and ideal power equation as follows:

$$P = \frac{{V_{out}}^2}{R_{load}} \quad (4.13)$$

$$R_{load} = \frac{400^2}{250} = 640\ ohms$$

Substituting this result back into equation 4.12 results in a critical inductance, L_{min} value of 623 μH.

The average current can be obtained from equation 4.4 as follows:

$$I_{L,avg} = \frac{3.5^2 \times \left(\frac{1 + 2 \times 0.31}{1 - 0.31}\right)^2 48}{640} = 5.2\ Amps$$

Solving the equation above we can obtain an $I_{L,avg}$ of 5.2 Amps

We have now designed the input inductor and it should have an inductance of 623 μH and must withstand of 5.2 Amps.

Using equation 4.5, the minimum capacitance value for the prototype converter can be obtained. The output voltage ripple here can be limited to 1 volt if the following is used:

$$C_{ox,min} = \frac{0.31}{2 \times 640\left(\frac{1}{400}\right)62.5 \times 10^3} = 1.55\ uF$$

The capacitor should be rated for 400 volts as that is output voltage seen by the component.

Now for the active components, the switch voltage stress can be computed based on equation 4.7

$$V_{Sx,max} = 48\left(\frac{1}{1 - 0.31}\right)$$

We can obtain a value of 70 volts for our switch voltage stress. Similarly, for our diodes we can use equation 4.9 and 4.10 to obtain values for the main and auxiliary diodes.

$$V_{D,main} = 3.5 \times 48\left(\frac{1}{1-0.31}\right)$$

$$V_{D,auxilliary} = 3.5 \times 48\left(\frac{1}{1-0.31}\right) - 3.5 \times 48$$

We can obtain diode voltage stresses of 243V and 76V.

The key parameters however need to be account for tolerances and availability of components, which makes accurate optimization difficult. Therefore, by factoring in tolerances we obtain the results can be summarized in table 4-2.

Table 4-2: Prototype key parameters

Duty cycle, D	0.31
Turns ratio, n	3.5
Switching frequency, f	50 kHz
Input inductor, L_{min}	650 μH
Output capacitance, C_{ox}	10 μF
Switch stress, $V_{sx,max}$	100 Volts
Main diode voltage stress, $V_{D,main}$	250 Volts
Auxiliary diode voltage stress, $V_{D,auxilliary}$	100 Volts

4.4 Experimental results

An experimental prototype of the proposed converter was implemented using the key parameters found in the design example. The key specifications are shown in table 4-3 for clarity.

Table 4-3: Prototype specifications

Input voltage, V_{in}	48 Volts
Output voltage, V_{out}	400 Volts
Power, P	250 Watt
Switching frequency, f	50 kHz

The experimental prototype was tested at full load with a duty cycle of 0.31 to obtain the required output voltage of 400 volts from a 48 volts DC supply with an efficiency of 88%.

4.4.1 Experimental setup

The prototype was realized using the following components.

- Switches: All switches S_1 - S_4 were Fairchild Semiconductor's FDP18N50, a standard N channel MOSFET fitted with ATS-PCBT1085 heatsinks

- Diodes: Secondary side diodes D_1 - D_4 were SMC diode SDURB830, ultrafast rectifier diodes. Input side diode, D_z was ST Microelectronics STPS30SM120S, a power Schottky rectifier.

- Inductor: Custom in-house designed inductor using Magnetic Inc's 77191a, a powder core toroid wound with 150 strands of 38AWG Litz wire

- Transformers: Custom in-house designed main transformer T_3 based on TDK ETD54 N87 core and accessories. The auxiliary transformers T_1 and T_2 were built on a TDK ETD29 N87 core and accessories.

- Capacitors: Input capacitors C_1 and C_2 were EPCOS B32776P, film capacitors. Output capacitors were Nichicon UCS2E101MHD electrolytic capacitors.

- Gate driver: Custom in-house design built on Texas Instruments UCC37321 MOSFET drivers and isolated power supplies to drive them based on Texas instruments DCP series isolated DC/DC converters.

- Controller: Custom in-house design based on the Atmel Atmega328P, a standard 8-bit microcontroller with hardware PWM. The embedded C code for the controller is provided in Appendix A.

4.4.2 Experimental Waveforms

Waveforms obtained from the prototype are shown and described in this section. Figure 4.7 below shows a typical input inductor current waveform. It can be seen that the input current rises and falls as does the input current in a conventional boost converter.

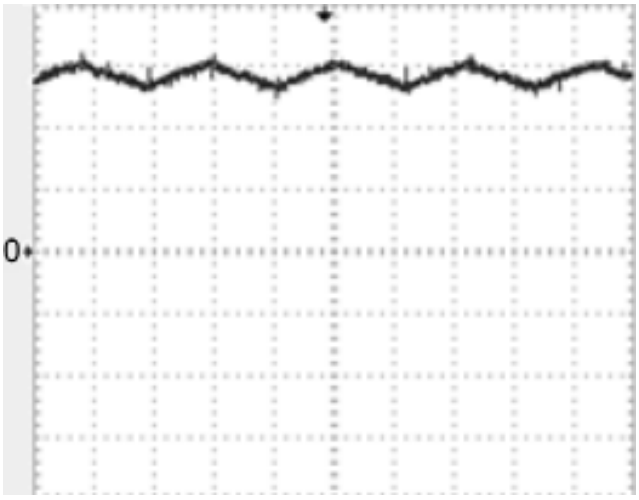

Figure 4.4: Typical inductor current, I_L [I_L: 2 A/div, t: 5µ/div]

Figure 4.8 shows the main transformer primary voltage waveform. It can be seen that this waveform is a square waveform with zero regions mixed with voltage regions. The zero regions occur when the DC bus is short-circuited and the voltage regions occur when the converter is in an energy transfer mode.

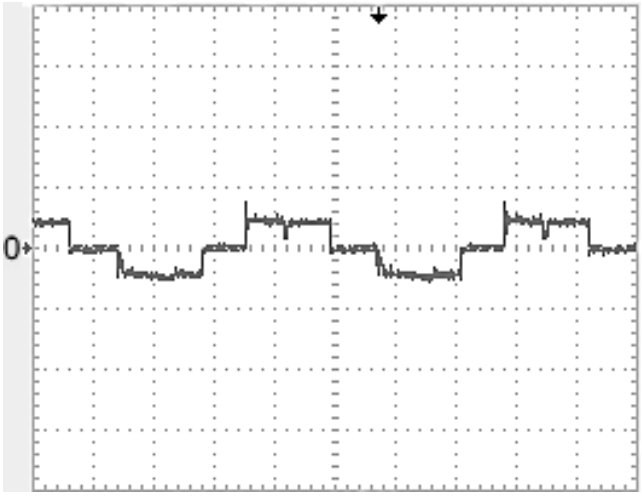

Figure 4.5: Main transformer voltage, $V_{T3, pri}$ [$V_{T3, pri}$: 200 V/div, t: 5µ/div]

Similar to Figure 4.8, Figure 4.9 shows the auxiliary transformer primary voltage waveform. It can be seen that this waveform is a square waveform again with zero regions mixed with voltage regions.

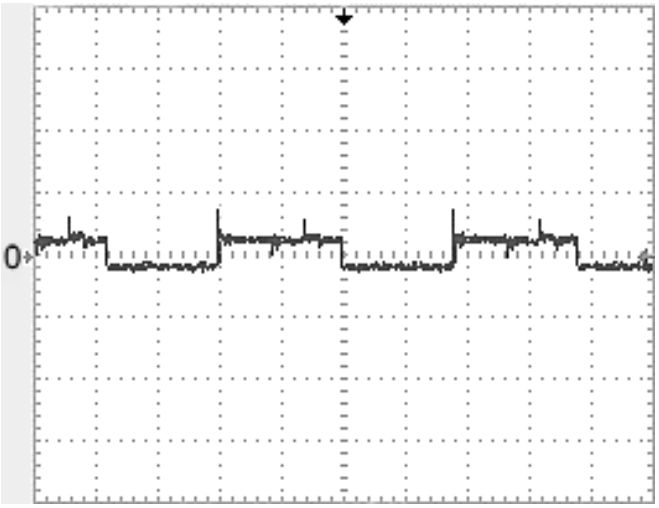

Figure 4.6: Auxiliary transformer voltage, $V_{T1, pri}$ [$V_{T1, pri}$: 50 V/div, t: 5µ/div]

Figure 4.10 shows the voltage across the main circuit output capacitor C_{o2} and the auxiliary circuit capacitor C_{o1}. From these figures it can be seen that the snubber circuit contributes to the total output voltage of the converter

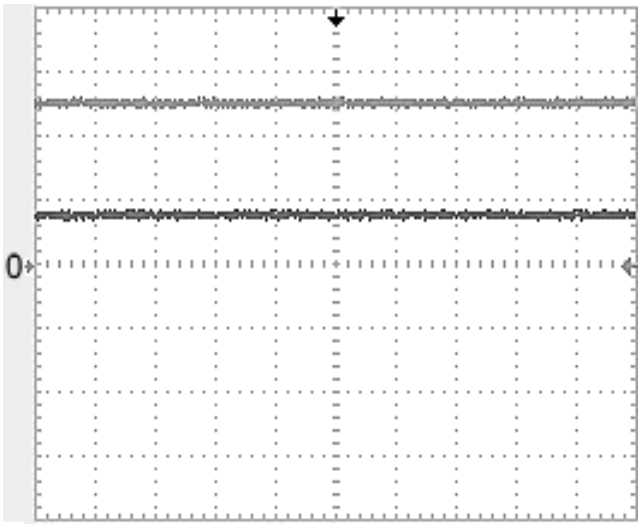

Figure 4.7: Voltage across the main and auxiliary circuit output capacitors, VC_{o1} and VC_{o2} [VC_{o1}, VC_{o2}: 100 V/div, t: 5µ/div]

4.5 Conclusion

The design of the converter was discussed in this chapter. The design process was discussed in detail and an example using this design process was illustrated. This was done to both to demonstrate the methodology used to ascertain the most important converter parameters and to verify the results of the analysis performed in chapter three. The results of the design process were used in the implementation of an experimental prototype converter that confirmed the feasibility of the converter.

Chapter 5

5 Conclusion

In this chapter, the contents of the thesis are summarized, the conclusions that have been reached based on the work performed in thesis are presented, and the main contributions of the thesis are stated. This chapter concludes by suggesting potential future research that can be done based on the thesis work.

5.1 Summary

High-gain DC-DC converters have become popular in recent years due to the considerable interest that has been generated by renewable energy systems. Renewable energy systems with photovoltaic (PV) solar panels and fuel cell stack inputs require some sort of power electronic converter interface to boost the voltage to a much higher DC level. This higher level DC voltage is then used to supply downstream converters such as DC-AC inverters that can feed power to the grid.

The objective of this thesis was to propose, analyze, design, implement and experimentally confirm the operation of a new high gain DC-DC full-bridge converter. The proposed converter was synthesized by modifying a current-fed full-bridge converter. The modifications that were made were: (i) taking a snubber circuit and modifying it by implementing the circuit with transformers instead of inductors; (ii) taking the transformer outputs and stacking them with the base current-fed full-bridge output; (iii) using this snubber circuit throughout a switching cycle as is done with the passive element network of a Z-source converter instead of just using the snubber circuit during switching transitions. A snubber circuit is needed in almost all power converters to clamp overvoltage spikes and it should be noted that the proposed converter uses the snubber circuit advantageously to increase the gain of the base current-fed converter.

In this thesis, a literature review of high gain DC-DC boost converters was carried out and their improvements and drawbacks were assessed to derive the proposed converter. The general operating principles of the converter were reviewed to explain its working and a steady-state analysis was performed on the key modes of operation. The results of the

analysis were used to generate graphs of characteristic curves of key converter components that were then used to develop a procedure for the design of the converter. This design procedure was then demonstrated with an example and the results of the design example were used in the construction of an experimental converter prototype that confirmed the feasibility of the proposed converter.

5.2 Converter Features

The main features of the proposed topology can be summarized as follows:

- The proposed converter has higher voltage gains without increasing the turns ratio of the transformers. As the energy from the snubber circuit is transferred to the output instead of circulating in the primary side, the converter can have a high voltage gain. The energy stored in the snubber capacitors is not dissipated through a resistor or a switch, as is the case with many passive snubbers. The energy is transferred to the output instead. This increase in gain is illustrated in Figure 5.1 below which compares the gain of the proposed converter with that of the conventional full bridge converter.

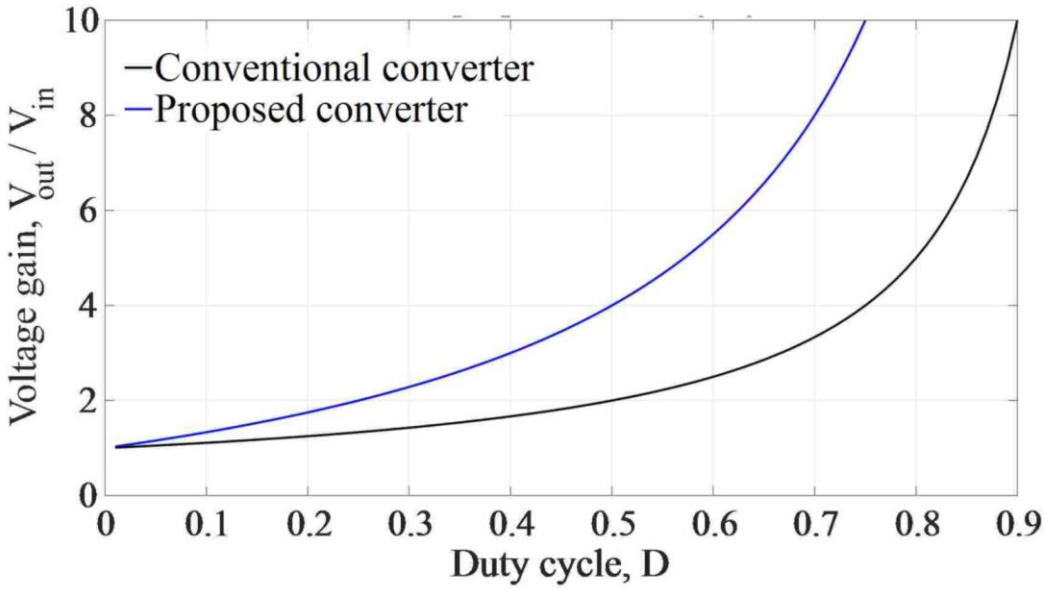

Figure 5.1: Voltage gain of proposed converter vs. conventional full bridge converter

- The converter's DC bus auxiliary circuit acts as a snubber that can clamp voltage spikes that would otherwise occur during the switching cycle of the converter, the DC bus capacitors also enable us to interface sources with voltage fluctuations.

- The overall current carried in the primary side of the transformer is lower due to the higher inherent gain of the proposed converter this reduces the complexity of the high frequency power transformer that is at the heart of an isolated DC-DC converter.

- The converter operates with standard PWM control and can be implemented with any commercially available PWM control IC.

- There is galvanic isolation between the low-side voltage and the high-side voltage. This isolation increases reliability and allows the use of this converter for applications where an isolated load needs to be driven.

- The converter is "open-circuit proof" as there is a path for current to flow through the auxiliary circuit if the converter switches somehow misfire and there is no available path for current to flow through. Current can flow through auxiliary circuit capacitors C_1 and C_2 and diode D_z until the converter switches return to normal operation. This increase the over all fault ride through capability of this converter

- The input current is continuous i.e. it is not chopped up during the switching cycle like other switched mode power supplies. This allows interfacing sensitive sources such as batteries without additional input side filters.

- Since the input current is continuous, the semiconductor peak current stresses are not excessive. The peak voltage and current stressed are comparable to other current fed full bridge DC-DC converters.

5.3 Contributions

The principal contributions of this thesis are as follows:

- A novel isolated high gain DC-DC converter topology with integrated passive snubber network was proposed in this thesis.
- The converter's steady-state operation was analyzed and key steady-state characteristics such as the effect of certain components on the operation of the converter were determined.
- A formal design procedure was developed to help power electronic personnel determine acceptable operation regions and design the converter.
- The feasibility of the converter was confirmed with simulation results obtained from PSIM, a popular, commercially available, power electronic simulation software package and with experimental results obtained from an experimental prototype converter.

5.4 Proposal for future work

- It is possible to step down voltage with the proposed converter by introducing open-zero states in the controller gate pulses. This is a feature that is not found in almost all high-gain DC-DC converters. This feature is useful as it allows the converter to be used in a wider range of applications. The voltage step-down operation of the proposed converter is something that can be investigated as part of future work
- As was stated in this thesis, the proposed converter can be used in renewable energy applications. The focus of the research presented in this thesis was on a particular power electronic converter. Future work can involve the study of a renewable energy system that is implemented with the proposed converter with a focus on the overall system instead of just the proposed converter.

References

[1] N. Mohan, *Power electronics : a first course*. Wiley, 2012.

[2] Y. Liu, H. Abu-Rub, B. Ge, F. Blaabjerg, O. Ellabban, and P. C. Loh, *Impedance source power electronic converters*. John Wiley & Sons, Ltd., 2016.

[3] P. C. Sen, *Power electronics*, 2nd ed. Nexus Special Interests, 1992.

[4] L. Yang, T. Liang, and J. Chen, "Transformerless DC–DC converters with high step-up voltage gain," *IEEE Transactions on Industrial Electronics*, vol. 56, no. 8, pp. 3144–3152, Aug. 2009.

[5] C. Y. Inaba, Y. Konishi, M. Nakamura, and M. Nakaoka, "High frequency PWM boost chopper-fed DC-DC converters with coupled-inductors," in *VIII IEEE International Power Electronics Congress, 2002. Technical Proceedings. CIEP 2002.*, pp. 134–138.

[6] M. Garg and R. K. Singh, "Coupled inductor boost converter with enhanced ESR filter capacitor for DC microgrid applications," in *2015 IEEE International Conference on Industrial Technology (ICIT)*, 2015, pp. 963–968.

[7] L. Zhu, "A Novel Soft-Commutating Isolated Boost Full-Bridge ZVS-PWM DC–DC Converter for Bidirectional High Power Applications," *IEEE Transactions on Power Electronics*, vol. 21, no. 2, pp. 422–429, Mar. 2006.

[8] A. Mousavi, P. Das, and G. Moschopoulos, "A Comparative Study of a New ZCS DC–DC Full-Bridge Boost Converter With a ZVS Active-Clamp Converter," *IEEE Transactions on Power Electronics*, vol. 27, no. 3, pp. 1347–1358, Mar. 2012.

[9] M. H. (Muhammad H. Rashid, *Power electronics handbook : devices, circuits, and applications*. Academic, 2006.

[10] D. W. Hart, *Power electronics*. McGraw-Hill, 2011.

[11] B. Akin, "An Improved ZVT–ZCT PWM DC–DC Boost Converter With Increased Efficiency," *IEEE Transactions on Power Electronics*, vol. 29, no. 4, pp. 1919–1926, Apr. 2014.

[12] H. Bodur and A. F. Bakan, "A new ZVT-PWM DC-DC converter," *IEEE Transactions on Power Electronics*, vol. 17, no. 1, pp. 40–47, 2002.

[13] T-W. Kim, H-S. Kim, and H-W. Ahn, "An improved ZVT PWM boost converter," in *2000 IEEE 31st Annual Power Electronics Specialists Conference.*, vol. 2, pp. 615–619.

[14] M. Esteki, M. Mohammadi, M. R. Yazdani, E. Adib, and H. Farzanehfard, "Family of soft-switching pulse-width modulation converters using coupled passive snubber," *IET Power Electronics*, vol. 10, no. 7, pp. 792–800, Jun. 2017.

[15] Q. Zhao and F. C. Lee, "High-efficiency, high step-up DC-DC converters," *IEEE Transactions on Power Electronics*, vol. 18, no. 1, pp. 65–73, Jan. 2003.

[16] E. Rodriguez, D. Abud, and J. Arau, “A novel single-stage single-phase DC uninterruptible power supply with power-factor correction,” *IEEE Transactions on Industrial Electronics*, vol. 46, no. 6, pp. 1137–1147, 1999.

[17] K-W. Ma and Y-S. Lee, “An integrated flyback converter for DC uninterruptible power supply,” *IEEE Transactions on Power Electronics*, vol. 11, no. 2, pp. 318–327, Mar. 1996.

[18] H. Zhang and F. Wang, “Powering a 35W DC Metal Halide High Intensity Discharge (HID) Lamp Based UCC3305,” *Modern Applied Science*, vol. 3, no. 12, p. 63, Nov. 2009.

[19] H. Ardi, A. Ajami, and M. Sabahi, “A Novel High Step-Up DC–DC Converter With Continuous Input Current Integrating Coupled Inductor for Renewable Energy Applications,” *IEEE Transactions on Industrial Electronics*, vol. 65, no. 2, pp. 1306–1315, Feb. 2018.

[20] X. Hu, B. Gao, Q. Wang, L. Li, and H. Chen, “A zero ripple input current boost converter for high gain applications,” *IEEE Journal of Emerging and Selected Topics in Power Electronics*, pp. 1–1, 2017.

[21] A. Torkan and M. Ehsani, “High step-up Z-source DC-DC converter with flyback and voltage multiplier,” in *2017 IEEE Applied Power Electronics Conference and Exposition (APEC)*, 2017, pp. 330–336.

[22] R. O. Caceres and I. Barbi, “A boost DC-AC converter: analysis, design, and experimentation,” *IEEE Transactions on Power Electronics*, vol. 14, no. 1, pp. 134–141, 1999.

[23] Ju-Won Baek, Myung-Hyo Ryoo, Tae-Jin Kim, Dong-Wook Yoo, and Jong-Soo Kim, “High boost converter using voltage multiplier,” in *31st Annual Conference of IEEE Industrial Electronics Society, 2005. IECON 2005.*, 2005.

[24] E. T. Calkin and B. H. Hamilton, “Circuit Techniques for Improving the Switching Loci of Transistor Switches in Switching Regulators,” *IEEE Transactions on Industry Applications*, vol. IA-12, no. 4, pp. 364–369, Jul. 1976.

[25] X. He, S. J. Finney, B. W. Williams, and T. C. Green, “An improved passive lossless turn-on and turn-off snubber,” in *Proceedings Eighth Annual Applied Power Electronics Conference and Exposition*, pp. 385–392.

[26] W. McMurray, “Optimum Snubbers for Power Semiconductors,” *IEEE Transactions on Industry Applications*, vol. IA-8, no. 5, pp. 593–600, Sep. 1972.

[27] P. Lauritzen and H. Smith, “A nondissipative snubber effective over a wide range of operating conditions,” in *1983 IEEE Power Electronics Specialists Conference*, 1983, pp. 345–354.

[28] P. C. Todd, “Snubber Circuits: Theory , Design and Application,” *Unitrode power electronics notes*, 1993.

[29] F. Z. Peng, “Z-source inverter,” in *Conference Record of the 2002 IEEE Industry Applications Conference. 37th IAS Annual Meeting (Cat. No.02CH37344)*, vol. 2, pp. 775–781.

[30] D. Vinnikov and I. Roasto, “Quasi-Z-Source-Based Isolated DC/DC Converters for Distributed Power Generation,” *IEEE Transactions on Industrial Electronics*, vol. 58, no. 1, pp. 192–201, Jan. 2011.

[31] Y. P. Siwakoti, F. Blaabjerg, P. C. Loh, and G. E. Town, “High-voltage boost quasi-Z-source isolated DC/DC converter,” *IET Power Electronics*, vol. 7, no. 9, pp. 2387–2395, Sep. 2014.

[32] X. Fang, Z. Chen, and X. Wang, “Current-Fed Quasi-Z-Source Inverter-Based Adjustable Speed Drive System With Bidirectional Power Flow,” *IEEE Transactions on Applied Superconductivity*, vol. 24, no. 5, pp. 1–6, Oct. 2014.

[33] Q. Lei, F. Z. Peng, and B. Ge, “Transient modeling of current-fed quasi-Z-source inverter,” in *2011 IEEE Energy Conversion Congress and Exposition*, 2011, pp. 2283–2287.

[34] X. Fang, “Maximum boost control of the current-fed Z-source inverter,” in *2008 IEEE International Conference on Industrial Technology*, 2008, pp. 1–6.

[35] F. Gao, P. C. Loh, F. Blaabjerg, and C. J. Gajanayake, “Operational analysis and comparative evaluation of embedded Z-Source inverters,” in *2008 IEEE Power Electronics Specialists Conference*, 2008, pp. 2757–2763.

[36] Y. Song and B. Wang, “Survey on Reliability of Power Electronic Systems,” *IEEE Transactions on Power Electronics*, vol. 28, no. 1, pp. 591–604, Jan. 2013.

[37] R. Wu, F. Blaabjerg, H. Wang, M. Liserre, and F. Iannuzzo, “Catastrophic failure and fault-tolerant design of IGBT power electronic converters - an overview,” in *IECON 2013 - 39th Annual Conference of the IEEE Industrial Electronics Society*, 2013, pp. 507–513.

[38] T. Funaki, “Comparative study of self turn-on phenomenon in high-voltage Si and SiC power MOSFETs,” *IEICE Electronics Express*, vol. 10, no. 21, Nov. 2013.

[39] Mag-Inc, “Magnetics - PFC Boost Design.” [Online]. Available: https://www.mag-inc.com/Products/Powder-Cores/Kool-Mu-Cores/PFC-Boost-Design. [Accessed: 16-Dec-2017].

[40] B. T. Lynch, “Under the Hood of a DC/DC Boost Converter,” 2008.

[41] S. W. Lee, “Practical Feedback Loop Analysis for Voltage-Mode Boost Converter,” 2014.

[42] S. Roberts, *DC/DC Book of Knowledge: Practical Tips for the User*. RECOM.

Appendices

Supplementary code and schematics are included in this section. It includes the controller code written in embedded C, MATLAB code used to plot Figure 3.3 and Figure 4.2 and the EagleCAD board layout and schematic used to fabricate the prototype converter.

Appendix A: Embedded C code

```
//Controller code to generate fast PWM pulses using counter 1 and 2 of
Atmel Atmega328

#include <avr/io.h>

int main(void)
{

    // Input

    float Ds=0.31; //Shoot through period duty cycle

    // Set timers and counters

    float Da=1-Ds; //Active period duty cycle

    Da=Da*256; //Convert to 8 bit active duty cycle

    TCNT1=127; // Phase shift value for 180 degree shift
    TCNT2=20; // Offset to obtain accurate 180 degree phase shift

    OCR1A = (int)Da; //Duty cycle variable for timer 1
    OCR1B = (int)Da; //Duty cycle variable for timer 1

    OCR2A = (int)Da; // Duty cycle variable timer 2
    OCR2B = (int)Da; // Duty cycle variable timer 2

    TCCR2A |= (1 << COM2A1); // set none-inverting mode
    TCCR2A |= (1 << COM2B1);

    TCCR2A |= (1 << WGM21) | (1 << WGM20);  // set fast PWM Mode

    TCCR2B |= (1 << CS20); // set no prescaler and starts PWM

    TCCR1A |= _BV(COM1A1) |_BV(COM1B1) | _BV(WGM10);
    TCCR1B |= _BV(CS10) | _BV(WGM12);

    // Assign PB1/OC1A/Timer1 ,PB2/OC1B/Timer1 and PB3/OC2A/Timer2
    DDRB |= _BV(PB1) | _BV(PB2) | _BV(PB3);
    DDRD |= _BV(PD3);
}
```

Appendix B: MATLAB code

```
%MATLAB code used to plot figure 3.3

clear all;
clc;

upperlimit=1;
lowerlimit=0;
delta=0.01;

number_of_steps=(upperlimit-lowerlimit)/delta;

d= zeros(1, round(number_of_steps));
gain_1= zeros(1, round(number_of_steps));
gain_5= zeros(1, round(number_of_steps));
gain_10= zeros(1, round(number_of_steps));

for n=1:number_of_steps

d(n)=(n)*delta;

gain_1(n)=((1+2*d(n))/(1-d(n)));

end

subplot(1,1,1)
plot(d,gain_1,'k')
hold on;
% plot(d,gain_5,'b')
% hold on;
% plot(d,gain_10,'r')
% hold on;

xlabel('Duty cycle, D_{s} '); ylabel('Voltage gain, V_{out} /
V_{in}');title('Voltage gain vs. duty cycle');
grid on;

% legend('show');
% legend('Turns ratio, n = 1','Turns ratio, n = 2','Turns ratio, n =
4');
% grid on;
```

```
%MATLAB code used to plot figure 4.2

clear all;
clc;

upperlimit=1;
lowerlimit=0;
delta=0.01;

number_of_steps=(upperlimit-lowerlimit)/delta;

d= zeros(1, round(number_of_steps));

gain_1= zeros(1, round(number_of_steps));

gain_2= zeros(1, round(number_of_steps));

gain_4= zeros(1, round(number_of_steps));

gain_6= zeros(1, round(number_of_steps));

gain_8= zeros(1, round(number_of_steps));

gain_10= zeros(1, round(number_of_steps));

for n=1:number_of_steps

d(n)=(n)*delta;

gain_1(n)=((1+2*d(n))/(1-d(n)));

end

for n=1:number_of_steps

d(n)=(n)*delta;

gain_2(n)=2*((1+2*d(n))/(1-d(n)));

end

for n=1:number_of_steps

d(n)=(n)*delta;

gain_4(n)=4*((1+2*d(n))/(1-d(n)));

end

for n=1:number_of_steps

d(n)=(n)*delta;

gain_6(n)=6*((1+2*d(n))/(1-d(n)));

end
```

```
for n=1:number_of_steps

d(n)=(n)*delta;

gain_8(n)=8*((1+2*d(n))/(1-d(n)));

end

for n=1:number_of_steps

d(n)=(n)*delta;

gain_10(n)=10*((1+2*d(n))/(1-d(n)));

end

subplot(1,1,1)
plot(d,gain_1,'k')
hold on;
plot(d,gain_2,'b')
hold on;
plot(d,gain_4,'r')
hold on;
plot(d,gain_6,'g')
hold on;
plot(d,gain_8,'y')
hold on;
plot(d,gain_10,'m')
hold on;

xlabel('Duty cycle, D_{s} '); ylabel('Voltage gain, V_{out} /
V_{in}');title('Voltage gain vs. duty cycle');
grid on;

legend('show');
legend('Turns ratio, n = 1','Turns ratio, n = 2','Turns ratio, n =
4','Turns ratio, n = 6','Turns ratio, n = 8','Turns ratio, n = 10');
grid on;
```

Curriculum Vitae

Name:	Prashanth Prabhu
Post-secondary Education and Degrees:	Manipal University Dubai, United Arab Emirates 2011-2015 B.Eng. University of Western Ontario London, Ontario, Canada 2016-2018 M.E.Sc.
Honors and Awards:	Academic excellence award 2012-2014
Related Work Experience	Design Engineer NSV Automotive 2015 - 2016

Publications:

[1] P. Prabhu, J. Khodabakhsh, M. Abo El Dahb, and G. Moschopoulos, "A High Gain DC-DC Full-Bridge Converter with Integrated Passive Snubber network," in *2017 International Communications Energy Conference(INTELEC)*, 2017.

[2] J. Khodabakhsh, P. Prabhu, and G. Moschopoulos, "Analysis and design of AC-DC resonant single-stage converter with reduced DC bus voltage variation," in *2017 International Communications Energy Conference(INTELEC)*, 2017.